by the NSF MRL Program through the Center for Materials Research at Stanford University. R.J.L. was supported by the NIH Medical Scientist Training Program at the Stanford University School of Medicine. D.E. was supported by NIH Grant 2 RO1 GM 31674 and a NIH Research Career Development Award 5 KO4 AM 01353. We acknowledge the valuable assistance of Susan Sorlie and Matheen Haleem.

References and Notes

(1) Fredericq, E.; Houssier, C. "Electric Dichroism and Electric Birefringence"; Clarendon Press: Oxford, 1973.
(2) Krause, S., Ed. "Molecular Electro-optics"; Plenum Press: New York, 1980.
(3) O'Konski, C. T., Ed. "Molecular Electro-optics"; Marcel Dekker: New York, 1976.
(4) Elias, J. G.; Eden, D. *Macromolecules* **1981**, *14*, 410.
(5) Elias, J. G.; Eden, D. *Biopolymers* **1981**, *20*, 2369.
(6) Hagerman, P. J. *Biopolymers* **1981**, *20*, 1503.
(7) Diekmann, S.; Hillen, W.; Morgeneyer, B.; Wells, R. D.; Porschke, D. *Biophys. Chem.* **1982**, *15*, 263.
(8) Stellwagen, N. C. *Biopolymers* **1981**, *20*, 399.
(9) Rau, D. C.; Bloomfield, V. A. *Biopolymers* **1979**, *18*, 2783.
(10) Stellwagen, N. C. *Biophys. Chem.* **1982**, *15*, 311.
(11) Marion, C.; Perrot, B.; Roux, B.; Bernengo, J. C. *Makromol. Chem.* **1984**, *185*, 1665.
(12) Marion, C.; Roux, B.; Bernengo, J. C. *Makromol. Chem.* **1984**, *185*, 1647.
(13) Yoshioka, K. *J. Chem. Phys.* **1983**, *79* (7), 3482.
(14) Diekmann, S.; Jung, M.; Teubner, M. *J. Chem. Phys.* **1984**, *80* (3), 1259.
(15) Wegener, W. A.; Dowben, R. M.; Koester, V. J. *J. Chem. Phys.* **1979**, *70* (2), 622.
(16) Rau, D. C.; Charney, E. *Macromolecules* **1983**, *16* (10), 982.
(17) Rau, D. C.; Charney, E. *Biophys. Chem.* **1983**, *7*, 35.
(18) Eden, D.; Elias, J. G. In "Measurement of Suspended Particles by Quasi-Elastic Light Scattering"; Dahneke, B. E., Ed.; Wiley: New York, 1983; p 401.
(19) Fixman, M. *Macromolecules* **1980**, *13*, 711.
(20) Fixman, M.; Jagannathan, S. *J. Chem. Phys.* **1981**, *75* (8), 4048.
(21) Hogan, M.; Dattagupta, N.; Crothers, D. M. *Proc. Natl. Acad. Sci. U.S.A.* **1978**, *75* (1), 195.
(22) Maret, G.; Weill, G. *Biopolymers* **1983**, *22*, 2727.
(23) Maniatis, T.; Fritsche, E. F.; Sambrook, J. "Molecular Cloning"; Cold Spring Harbor Laboratory: Cold Spring Harbor, New york, 1982.
(24) Lewis, R. J.; Huang, J. H.; Pecora, R. *Macromolecules* **1985**, *18*, 1530.
(25) Tirado, M. M.; Martinez, C. L.; Garcia de la Torre, J. *J. Chem. Phys.* **1984**, *81* (4), 2047.
(26) Broersma, S. *J. Chem. Phys.* **1981**, *74*, 6989.
(27) Broersma, S. *J. Chem. Phys.* **1960**, *32*, 1626.
(28) Broersma, S. *J. Chem. Phys.* **1960**, *32*, 1632.
(29) Tirado, M. M.; Garcia de la Torre, J. *J. Chem. Phys.* **1979**, *71*, 2581.
(30) Stimpson, D. I.; Bloomfield, V. A. *Biopolymers* **1985**, *24*, 387.
(31) Tirado, M. M.; Garcia de la Torre, J. *J. Chem. Phys.* **1980**, *73*, 1986.
(32) Newman, J.; Swinney, H. L.; Day, L. A. *J. Mol. Biol.* **1977**, *116*, 593.
(33) Hagerman, P. J.; Zimm, B. H. *Biopolymers* **1981**, *20*, 1481.
(34) Hearst, J. E. *J. Chem. Phys.* **1963**, *38* (5), 1062.
(35) Provencher, S. W. *Biophys. J.* **1976**, *16*, 27.
(36) Provencher, S. W. *J. Chem. Phys.* **1976**, *64*, 2772.
(37) Provencher, S. W.; Hendrix, J.; De Maeyer, L.; Paulussen, N. *J. Chem. Phys.* **1978**, *69* (9), 4273.
(38) Provencher, S. W. *Makromol. Chem.* **1979**, *180*, 201.
(39) Provencher, S. W. "CONTIN User's Manual"; European Molecular Biology Laboratory Technical Report EMBL-DAO2, Heidelberg, 1980.
(40) Roitman, D. B.; Zimm, B. H. *J. Chem. Phys.* **1984**, *81* (12), 6348.
(41) Roitman, D. B. *J. Chem. Phys.* **1984**, *81* (12), 6356.
(42) Roitman, D. B.; Zimm, B. H. *J. Chem. Phys.* **1984**, *81* (12), 6333.
(43) Hassager, O. *J. Chem. Phys.* **1974**, *60* (5), 2111.
(44) Hassager, O. *J. Chem. Phys.* **1974**, *60* (10), 4001.
(45) Aragón, S. R.; Pecora, R. *Macromolecules* **1985**, *18*, 1868.
(46) Zimm, B. H. *J. Chem. Phys.* **1956**, *24* (2), 269.
(47) Zimm, B. H.; Roe, G. M.; Epstein, L. F. *J. Chem. Phys.* **1956**, *24* (2), 279.
(48) Harrington, R. E. *Biopolymers* **1978**, *17*, 919.
(49) Highsmith, S.; Eden, D. *Biochemistry*, in press.
(50) Lewis, R. J., unpublished data.
(51) Lewis, R. J.; Huang, J. H.; Pecora, R. *Macromolecues*, **1985**, *18*, 944.
(52) Dickerson, R. E. *Sci. Am.* **1983**, *249* (6), 94.
(53) Hagerman, P. J. *Biopolymers* **1983**, *22*, 811.

Atomistic Modeling of Mechanical Properties of Polymeric Glasses

Doros N. Theodorou and Ulrich W. Suter*

Department of Chemical Engineering, Massachusetts Institute of Technology, Cambridge, Massachusetts 02139. *Received June 5, 1985*

ABSTRACT: Methods are developed for the prediction of the elastic constants of an amorphous glassy polymer by small-strain deformation of microscopically detailed model structures. A thermodynamic analysis shows that entropic contributions to the elastic response to deformation can be neglected in polymeric glasses. A statistical mechanical analysis further indicates that vibrational contributions of the hard degrees of freedom are not significant, so that estimates of the elastic constants can be obtained from changes in the total potential energy of static microscopic structures subjected to simple deformations. Mathematical procedures are developed for the atomistic modeling of deformation and applied to glassy atactic polypropylene. Predicted elastic constants are always within 15% of the experimental values, without the use of adjustable parameters. An estimate of the thermal expansion coefficient is also obtained. Inter- and intramolecular contributions to the mechanical properties are examined, and it is found that coexistence in the bulk reduces the effects of individual chain idiosyncrasy.

Introduction

A method for the detailed, atomistic modeling of well-relaxed amorphous glassy polymers has recently been introduced.[1] The polymeric glass was pictured as an ensemble of static microscopic structures in detailed mechanical equilibrium (but not in thermodynamic equilibrium), each microscopic structure being represented by a model cube with periodic boundaries, filled with segments from a single "parent chain". Our modeling approach was applied to glassy atactic polypropylene with very satisfactory results. Model estimates of the cohesive energy and of Hildebrand's solubility parameter agreed very well

* Address correspondence to MIT Chemical Engineering Department, Room 66-456, Cambridge, MA 02139.

0024-9297/86/2219-0139$01.50/0

with experiment. Single-chain conformation was found to be essentially unperturbed and long-range order to be completely absent.

We not turn to an investigation of the response of the detailed atomistic models to deformation and hence to the theoretical estimation of *macroscopic mechanical properties of glasses from first principles.*

Little has been published on this subject to date. Previous publications pertain almost exclusively to the crystalline state, in which the existence of a well-defined periodic structure permits considerable simplification. A statistical mechanical treatment of crystalline polymethylene by Pastine[2] led to a P–V–T equation of state that compares favorably with experiment, and Tashiro, Kobayashi, and Tadokoro[3,4] derived elastic constants for a variety of crystalline polymers. Mechanical properties of glassy amorphous polymers have not yet been deduced from their detailed molecular structure, but a number of correlations exist. The assumption of a Lennard-Jones-like relationship between total potential energy and the linear dimensions of a sample led Haward and MacCallum[5] to a successful correlation between adiabatic compressibility and molar volume. Schuyer (p 267 of ref 6) used group contribution methods to arrive at an estimate of the compressibility; tensile and shear moduli can be obtained from the compressibility by using an estimate for the Poisson ratio.

Yannas[7,8] considered displacements, on the molecular level, brought about by mechanical deformation of glassy polymers and found that the primary molecular mechanism is by rotation around skeletal bonds rather than by distortion of bond angles or bond distances. He introduced the term "strophon" for a segment three virtual bonds long. Inter- and intramolecular contributions to deformation were considered separately.

Recently, an atomistic approach to plastic deformation in amorphous metals has been introduced by Maeda and Takeuchi[9] and by Srolovitz, Vitek, and Egami.[10] The work presented here, although developed completely independently and referring to bonded systems, small deformations, and nonzero temperatures, has certain aspects in common with their approach.

Thermodynamic Considerations

A body can be regarded (Chapter 1 of ref 11) as a collection of particles whose positions are denoted by $\mathbf{r}_0 = (r_{0,1}, r_{0,2}, r_{0,3}) \equiv (x_0, y_0, z_0)$ in the reference (undeformed) state and by $\mathbf{r} = (r_1, r_2, r_3) \equiv (x, y, z)$ in the deformed state. The vector $\mathbf{s}$ with components $s_i = r_i - r_{0,i}$ is the "displacement vector". The material strain tensor ϵ is defined by

$$\epsilon_{LM} = \frac{1}{2}\left(\sum_{i=1}^{3} \frac{\partial r_i}{\partial r_{0,L}} \frac{\partial r_i}{\partial r_{0,M}} - \delta_{LM}\right) = \frac{1}{2}\left(\frac{\partial s_L}{\partial r_{0,M}} + \frac{\partial s_M}{\partial r_{0,L}}\right) + \frac{1}{2}\left(\sum_{i=1}^{3} \frac{\partial s_i}{\partial r_{0,M}} \frac{\partial s_i}{\partial r_{0,L}}\right) \quad (1)$$

We are only concerned with very small deformations. Terms of second order in the derivatives of displacement with respect to position will therefore be neglected in defining ϵ, and material and spatial strain will be considered identical (Chapter 13 or ref 12).

The material stress tensor is denoted by τ. As for the strain, material and spatial stress are not distinguished. The element τ_{LM} is taken equal to the force per unit area acting on an element of surface perpendicular to axis L and along the direction M. If $\mathbf{dF}$ is the surface force on an element of surface dS, where the exterior unit normal is $\mathbf{n}$, we write in matrix notation

$$\mathbf{dF} = \tau^T \mathbf{n}\, \mathrm{dS} \quad (2)$$

The terms ϵ and τ are symmetric and can also be represented, in Voigt notation, as vectors of six components (p 14 of ref 11). The two notations will be used interchangeably; which of the two notations is employed will be evident from the number of subscripts:

$$\epsilon_1 = \epsilon_{11}, \quad \epsilon_2 = \epsilon_{22}, \quad \epsilon_3 = \epsilon_{33}, \quad \epsilon_4 = 2\epsilon_{23}, \quad \epsilon_5 = 2\epsilon_{31}, \quad \epsilon_6 = 2\epsilon_{12} \quad (3a)$$

$$\tau_1 = \tau_{11}, \quad \tau_2 = \tau_{22}, \quad \tau_3 = \tau_{33}, \quad \tau_4 = \tau_{23}, \quad \tau_5 = \tau_{31}, \quad \tau_6 = \tau_{12} \quad (3b)$$

The fundamental thermodynamic equation for an elastic system in terms of the stress and strain tensors, at constant chemical composition, assumes the form

$$\mathrm{d}U = T\,\mathrm{d}S + V_0 \sum_{LM} \tau_{LM}\, \mathrm{d}\epsilon_{LM} = T\,\mathrm{d}S + V_0 \sum_{I} \tau_I\, \mathrm{d}\epsilon_I \quad (4)$$

(the subscript 0 denotes the undeformed state). For the Helmholtz energy ($A = U - TS$) we obtain, in differential form

$$\mathrm{d}A = -S\,\mathrm{d}T + V_0 \sum_{LM} \tau_{LM}\, \mathrm{d}\epsilon_{LM} = -S\,\mathrm{d}T + V_0 \sum_{I} \tau_I\, \mathrm{d}\epsilon_I \quad (5)$$

The (fourth-order) tensor of isothermal elastic coefficients is defined by

$$C_{LMNK} = \left.\frac{\partial \tau_{LM}}{\partial \epsilon_{NK}}\right|_{T,\epsilon_{(NK)}} = \frac{1}{V_0} \left.\frac{\partial^2 A}{\partial \epsilon_{LM} \partial \epsilon_{NK}}\right|_{T,\epsilon_{(LM,NK)}} \quad (6)$$

As a result of the Voigt symmetry relationships (p 32 of ref 11), eq 6 can be condensed into a symmetric 6×6 matrix, $\mathbf{C}$. For an isotropic material, such as an amorphous glassy polymer, eq 6 then assumes the form

$$\mathbf{C} = \begin{bmatrix} 2\mu + \lambda & \lambda & \lambda & 0 & 0 & 0 \\ \lambda & 2\mu + \lambda & \lambda & 0 & 0 & 0 \\ \lambda & \lambda & 2\mu + \lambda & 0 & 0 & 0 \\ 0 & 0 & 0 & \mu & 0 & 0 \\ 0 & 0 & 0 & 0 & \mu & 0 \\ 0 & 0 & 0 & 0 & 0 & \mu \end{bmatrix} \quad (7)$$

where λ and μ are the Lamé constants. The tensile (Young's) modulus, E, the shear modulus, G, the bulk modulus, B, and the Poisson ratio, ν, are related to λ and μ by

$$E = \mu\frac{3\lambda + 2\mu}{\lambda + \mu} \qquad G = \mu$$
$$B = \frac{1}{\kappa_T} = \lambda + \frac{2}{3}\mu \qquad \nu = \frac{\lambda}{2(\lambda + \mu)} \quad (8)$$

The strain dependence of the entropy, at constant temperature, is given (p 34 of ref 11) by the Grüneisen tensor γ

$$\gamma_{LM} = \frac{1}{\rho_0 c_\epsilon V_0} \left.\frac{\partial S}{\partial \epsilon_{LM}}\right|_{T,\epsilon_{(LM)}} = -\frac{1}{\rho_0 c_\epsilon} \left.\frac{\partial \tau_{LM}}{\partial T}\right|_{\epsilon} \quad (9)$$

where c_ϵ is the heat capacity per unit mass of material at constant strain. (The tensor γ could again be represented in condensed notation.) For an isotropic solid

$$\gamma_{LM} = \gamma \delta_{LM} = \frac{1}{\rho_0 c_\epsilon} \frac{\alpha_p}{\kappa_T} \quad (10)$$

where α_p is the volumetric thermal expansion coefficient and γ the "Grüneisen parameter".

Consider now an arbitrary elastic solid subjected to an arbitrary isothermal small deformation. Expanding the

internal energy, U, into a Taylor series around the undeformed state, to second order, and using the definitions introduced above, we obtain

$$U = A + TS = U_0 + V_0\sum_{LM}[\tau_{LM} + \rho_0 c_\epsilon T\gamma_{LM}]\epsilon_{LM} + \frac{1}{2}V_0\sum_{LMNK}\sum\left[C_{LMNK} - T\frac{\partial}{\partial T}C_{LMNK}\Big|_\epsilon\right]\epsilon_{LM}\epsilon_{NK} \quad (11)$$

The first terms in the brackets are due to the strain derivatives of the Helmholtz energy; the second terms originate in the corresponding derivatives of the entropy. The quantity

$$\frac{1}{3}\mathrm{Tr}(\tau + \rho_0 c_\epsilon T\gamma) = -P + \frac{\alpha_p T}{\kappa_T} = \frac{\partial U}{\partial V}\Big|_T$$

is sometimes termed "internal pressure". By analogy we will call the tensor

$$\sigma = \tau + \rho_0 c_\epsilon T\gamma \quad (12)$$

the "internal stress tensor".

We now focus on the second-order term in (11) in order to assess the relative importance of the contributions of internal energy and entropy to the elastic coefficients:

$$V_0 C_{LMNK} = \frac{\partial^2 A}{\partial\epsilon_{LM}\partial\epsilon_{NK}}\Big|_{T,\epsilon(LM,NK)} = \frac{\partial^2 U}{\partial\epsilon_{LM}\partial\epsilon_{NK}}\Big|_{T,\epsilon(LM,NK)} - T\frac{\partial^2 S}{\partial\epsilon_{LM}\partial\epsilon_{NK}}\Big|_{T,\epsilon(LM,NK)} = \frac{\partial^2 U}{\partial\epsilon_{LM}\partial\epsilon_{NK}}\Big|_{T,\epsilon(LM,NK)} - T\frac{\partial}{\partial T}C_{LMNK}\Big|_\epsilon \quad (13)$$

Entropic effects are relatively unimportant if the dimensionless ratio

$$\left|\frac{1}{C_{LMNK}}\left(T\frac{\partial C_{LMNK}}{\partial T}\Big|_\epsilon\right)\right| = \left|\frac{\partial \ln C_{LMNK}}{\partial \ln T}\Big|_\epsilon\right| \ll 1 \quad (14)$$

Temperature derivatives of the elastic coefficients at constant strain are not usually available experimentally. For an isotropic solid, and under the condition that the reference (undeformed) state is characterized by an isotropic stress distribution, (14) can be transformed to (see Appendix A)

$$\left|\frac{1}{C_{LMNK}}\left[T\frac{\partial C_{LMNK}}{\partial T}\Big|_P + \frac{\alpha_p T}{\kappa T}\frac{\partial C_{LMNK}}{\partial P}\Big|_T\right]\right| \ll 1 \quad (15)$$

For uniform hydrostatic compression the relevant elastic constant is

$$B = C_{11} + C_{22} + C_{33} + 2C_{23} + 2C_{31} + 2C_{12}$$

From (15) we obtain

$$\left|\frac{1}{B}\left[T\frac{\partial B}{\partial T}\Big|_P + \alpha_P T B\frac{\partial B}{\partial P}\Big|_T\right]\right| \ll 1$$

or

$$\left|\frac{T}{\kappa_T}\frac{\partial \kappa_T}{\partial T}\Big|_P + \frac{\alpha_P T}{\kappa_T{}^2}\frac{\partial \kappa_T}{\partial P}\Big|_T\right| \ll 1 \quad (16)$$

For pure shear, e.g., perpendicular to z and in the direction x, the relevant elastic constant is $C_{3131} = C_{55} = \mu = G$. Then (15) is

$$\left|\frac{T}{G}\frac{\partial G}{\partial T}\Big|_P + \frac{\alpha_P T}{\kappa_T}\frac{1}{G}\frac{\partial G}{\partial P}\Big|_T\right| \ll 1 \quad (17)$$

Koppelmann, Leder, and Royer[13] have obtained a set of excellent experimental values for the test of criteria in (16) and (17) for a typical glass. Their measurements on glassy PMMA at $T = 20$ °C, $P = 1$ atm, and a frequency of 4 MHz lead to $\alpha_P = 18.7 \times 10^{-5}$ K^{-1}, $\kappa_T = 1.70 \times 10^{-4}$ MPa^{-1}, $G = 1.88 \times 10^3$ MPA, $(\partial\kappa_T/\partial P)|_T = -1.59 \times 10^{-7}$ MPa^{-2}, $(\partial\kappa_T/\partial T)|_P = 2.16 \times 10^{-7}$ MPa^{-1} K^{-1}, $(\partial G/\partial P)|_T = 3.44$, $(\partial G/\partial T)|_P = -4.69$ MPa K^{-1} and hence to

$$\left|\frac{T}{\kappa_T}\frac{\partial \kappa_T}{\partial T}\Big|_P + \frac{\alpha_P T}{\kappa_T{}^2}\frac{\partial \kappa_T}{\partial P}\Big|_T\right| = 0.071 \ll 1$$

$$\left|\frac{T}{G}\frac{\partial G}{\partial T}\Big|_P + \frac{\alpha_P T}{\kappa_T}\frac{1}{G}\frac{\partial G}{\partial P}\Big|_T\right| = 0.14 \ll 1 \quad (18)$$

The criteria in (16) and (17) are satisfied for an amorphous polymer below its glass-formation temperature (far from frequency regions in which dynamic transitions are observed).

The thermodynamic analysis has shown that the internal energy contribution to the elastic response to deformation is much more significant than the entropic contribution. Below we therefore concentrate on the internal energy contribution only.

Statistical Mechanical Considerations

General Formulation. Consider a system of polymer chains within a cube of volume V filled with bulk amorphous polymer. For simplicity periodic boundary conditions are imposed, and the contents of the cube are obtained from a single "parent chain" of the type $CH_3CHR(CH_2CHR)_{x-1}CH_3$, where CH_3 and R are simple nonarticulated "pseudo-atoms".[1]

A complete microscopic description of the system in configuration space is given by specifying (a) all $6x - 2$ bond lengths in the system, collectively denoted by $\mathbf{l}$; (b) all $10x - 5$ independent bond (valence) angles in the system, collectively denoted by their complements θ; (c) the location of the chain start, $\mathbf{r}_{c_0}$; (d) the "Euler angles" $\psi = (\psi_1, \psi_2, \psi_3)$, specifying the overall orientation of the parent chain with respect to a fixed frame of reference; and (e) all $2x - 2$ torsion angles $\varphi = (\varphi_2, \varphi_3, ..., \varphi_{2x-1})$ of all bonds of the chain but the first and last. Variables $\mathbf{r}_{c_0}$ and ψ are "external", while variables φ, $\mathbf{l}$, and θ are "internal". Variables $\mathbf{r}_{c_0}$, ψ, and φ are considered to be "soft", whereas variables $\mathbf{l}$ and θ are thought to be "hard". The total number of soft variables in the system is $N_s = 2x + 4$; that of hard variables is $N_h = 16x - 7$. The total number of atoms is $N = 6x - 1 = (1/3)(N_s + N_h)$.

To describe the system in momentum space, one needs another $3N$ variables, so that the overall phase space of our system is $(36x - 6)$-dimensional.

A detailed analysis of the partition function in a polymer system has been given by Gō and Scheraga,[14] who found that motion associated with the soft degrees of freedom can be treated classically, whereas (vibrational) motion associated with the hard degrees of freedom must be treated quantum mechanically. Extending their single-chain analysis to the bulk polymer, we can write the general ("exact") partition function of our system as

$$Z = \left(\frac{1}{2\pi\beta\hbar^2}\right)^{N_s/2} V\{\sum_{k=1}^{N} m_k\}^{3/2} \times \int\left[\prod_{i=1}^{N_h}\left(\frac{\exp\left(-\frac{\beta\hbar\omega_i}{2}\right)}{1 - \exp(-\beta\hbar\omega_i)}\right)\right]\left[\frac{1}{\det \mathbf{G}}\right]^{1/2} \times \exp[-\beta U^{\mathrm{pot}}(\psi, \varphi)]\, d\psi\, d\varphi \quad (19)$$

where $\beta = 1/k_B T$. The first factor in the above expression

arises from the momentum integration of the soft variables, treated classically. The volume is due to integration over $\mathbf{r}_{c_0}$, while the term involving frequencies originates in the quantum treatment of the hard degrees of freedom. The quantity $U^{pot}(\psi, \varphi)$ denotes the total potential energy as a function of Euler and torsion angles, with all hard variables kept fixed at their equilibrium positions. $\mathbf{G}$ is a transformation matrix, depending on the atomic masses and the system configuration, that stems from the transformation from a representation in terms of Cartesian coordinates to a representation in internal variables

$$(\mathbf{G}^{-1})_{ij} = \sum_{k=1}^{N} \sum_{\alpha=1}^{3} m_k \frac{\partial r_{k,\alpha}}{\partial q_i} \frac{\partial r_{k,\alpha}}{\partial q_j} \tag{20}$$

where m_k and $r_{k,\alpha}$ denote the mass and Cartesian coordinates of atom k and $\mathbf{q} = [\psi^T \varphi^T]^T$ is the $(N_s - 3)$-dimensional vector of Euler and rotation angles.

The thermodynamics of a multichain polymer system in equilibrium can be deduced, in principle, from the partition function within the framework of the canonical ensemble. The Helmholtz energy, A, and internal energy, U, are simply related to Z by

$$A = -\frac{1}{\beta} \ln Z \qquad U = -\frac{\partial \ln Z}{\partial \beta} \tag{21}$$

Harmonic Approximation. A polymeric glass is not in thermodynamic equilibrium and does not have free access to all of configuration space. At temperatures $T \leq T_g - 20$ °C, which are of interest in this work, polymeric glasses are solids for all practical purposes. Characteristic times for volume relaxation are of the order of years (p 387 of ref 15). Thermal motion consists predominantly of solidlike vibrations of atoms around their average equilibrium positions (p 14 of ref 16), and mechanical response to small deformations is adequately described by linear elasticity (p 108 of ref 17).

For the purpose of modeling this "solidlike" elastic response of a glass to small deformation, we consider it to be confined to the vicinity of a local minimum of the total potential energy in configuration space. We symbolize that minimum as $U^{pot}_{min} = U^{pot}(\psi_{min}, \varphi_{min})$.

"Quasi-thermodynamic" relationships around this minimum can be written as would be done for a crystalline solid. Expanding the function $U^{pot}(\psi, \varphi)$ around $(\psi_{min}, \varphi_{min})$, we get

$$U^{pot}(\psi, \varphi) = U^{pot}_{min} + \mathbf{g}_{min}{}^T \begin{bmatrix} \Delta\psi \\ \Delta\varphi \end{bmatrix} + \frac{1}{2}\left[\Delta\psi^T \Delta\varphi^T\right] \mathbf{H}_{min} \begin{bmatrix} \Delta\psi \\ \Delta\varphi \end{bmatrix} \tag{22}$$

where $\Delta\psi = \psi - \psi_{min}$, $\Delta\varphi = \varphi - \varphi_{min}$, the gradient $\mathbf{g}_{min} = \mathbf{g}(\psi_{min}, \varphi_{min})$, and the Hessian $\mathbf{H}_{min} = \mathbf{H}(\psi_{min}, \varphi_{min})$.

Analytical expressions for the $(N_s - 3)$-dimensional gradient $\mathbf{g}(\psi, \varphi)$ and the $(N_s - 3) \times (N_s - 3)$-dimensional Hessian $\mathbf{H}(\psi, \varphi)$ have been given previously.[1] By definition $\mathbf{g}_{min} = \mathbf{0}$, $\mathbf{H}_{min}$ is positive definite, and, from (22)

$$U^{pot}(\psi, \varphi) = U^{pot}_{min} + \frac{1}{2}\left[\Delta\psi^T \Delta\varphi^T\right] \mathbf{H}_{min} \begin{bmatrix} \Delta\psi \\ \Delta\varphi \end{bmatrix} \tag{23}$$

We assume that all contributions to the integral in (19) come from the vicinity of $(\psi_{min}, \varphi_{min})$. Furthermore, we conjecture that $\mathbf{G}$ and the frequencies ω_i do not vary very much with ψ and φ near this minimum, so that they can be assumed constant. Then, using (23) in (19), we obtain (p 310 in ref 18)

$$Z = \left(\frac{1}{2\pi\beta\hbar^2}\right)^{N_s/2} V\{\sum_{k=1}^{N} m_k\}^{3/2} \times \prod_{i=1}^{N_h}\left[\frac{\exp\left(-\frac{\beta\hbar\omega_i}{2}\right)}{1 - \exp(-\beta\hbar\omega_i)}\right]\left[\frac{1}{\det \mathbf{G}_{min}}\right]^{1/2} \times \left(\frac{2\pi}{\beta}\right)^{(N_s-3)/2}\left[\frac{1}{\det \mathbf{H}_{min}}\right]^{1/2} \exp(-\beta U^{pot}_{min}) = \left(\frac{\sum_{k=1}^{N} m_k}{2\pi\beta\hbar^2}\right)^{3/2}\left(\frac{1}{\beta\hbar}\right)^{N_s-3}\left[\frac{V^2}{\det(\mathbf{G}_{min}\mathbf{H}_{min})}\right]^{1/2} \times \prod_{i=1}^{N_h}\frac{\exp\left(-\frac{\beta\hbar\omega_i}{2}\right)}{1 - \exp(-\beta\hbar\omega_i)} \exp(-\beta U^{pot}_{min}) \tag{24}$$

The last three factors in (23) incorporate the spatial dependence of the partition function. From (21)

$$A = U^{pot}_{min} + \frac{1}{2\beta} \ln\left[\frac{\det(\mathbf{G}_{min}\mathbf{H}_{min})}{V^2}\right] - \frac{1}{\beta} \ln\left[\left(\frac{\sum_{k=1}^{N} m_k}{2\pi\beta\hbar^2}\right)^{3/2}\left(\frac{1}{\beta\hbar}\right)^{N_s-3}\right] + A_{vib} \tag{25}$$

$$U = U^{pot}_{min} + \left(N_s - \frac{3}{2}\right)\frac{1}{\beta} + U_{vib} \tag{26}$$

where

$$A_{vib} = -\frac{1}{\beta} \ln Z_{vib}$$

$$U_{vib} = -\frac{\partial \ln Z_{vib}}{\partial \beta} \tag{27}$$

$$Z_{vib} = \prod_{i=1}^{N_h} \frac{\exp\left(-\frac{\beta\hbar\omega_i}{2}\right)}{1 - \exp(-\beta\hbar\omega_i)}$$

Let ξ be any space-related quantity (such as volume or a strain component). We concentrate on the derivative $(\partial U/\partial\xi)|_T$ (internal pressure and internal stress tensor; compare eq 12) and $(\partial^2 A/\partial\xi^2)|_T$ (bulk modulus of elasticity and isothermal elastic coefficients; compare eq 13). From (25) and (26) we have

$$\left.\frac{\partial U}{\partial \xi}\right|_T = \left.\frac{\partial U^{pot}_{min}}{\partial \xi}\right|_T + \left.\frac{\partial U_{vib}}{\partial \xi}\right|_T \tag{28}$$

$$\left.\frac{\partial^2 A}{\partial \xi^2}\right|_T = \left.\frac{\partial^2 U^{pot}_{min}}{\partial \xi^2}\right|_T + \frac{1}{2\beta}\frac{\partial}{\partial \xi} \ln\left[\frac{\det(\mathbf{G}_{min}\mathbf{H}_{min})}{V^2}\right]\Bigg|_T + \left.\frac{\partial^2 A_{vib}}{\partial \xi^2}\right|_T \tag{29}$$

Equation 28 expresses the fact that only that part of the kinetic energy which is associated with the hard-mode vibrations is spatially dependent. The contribution of the soft degrees of freedom, treated classically, amounts to an equipartition term (eq 26), which does not depend on ξ.

Equation 29, which is actually the "quasi-harmonic approximation" (p 14 of ref 11) applied to glassy amorphous polymers, breaks up the elastic constant into three terms:

The first term consists of a "potential energy contribution". It expresses the dependence of the energy of the minimum, to which our system is confined, to changes in the spatial extent and shape of the system.

The second term incorporates a "configurational entropy" contribution. It depends on the curvature ($\mathbf{H}_{min}$) of the potential energy hypersurface around the minimum and can be used to assess the importance of entropy effects on the elastic constants. Above we have deduced that these effects are not significant, and this term will be *neglected* in the following. This corresponds to the "strict harmonic approximation" (p 141 of ref 11) for the soft degrees of freedom.

The third term gives the volume dependence and strain dependence of the vibrational frequencies associated with the hard degrees of freedom. By neglecting the configurational entropy term in (29), we are left only with potential energy and vibrational contributions in each of (28) and (29). The significance of vibrational contributions is examined next for $\xi = V$.

Vibrational Contributions. The vibrational terms in (28) and (29) could, in principle, be evaluated exactly by detailed consideration of all normal modes (p 179 in ref 27 and ref 2) in our system. Such an exact treatment in a disordered multichain system exceeds current abilities, however. We only estimate the significance of "hard" vibrational contributions based on two limiting models that are frequently used for solid polymers: the Einstein model and the Debye model. Each of these models assumes a specific distribution for the vibrational frequencies, ω_i, in the vibrational partition function (eq 27), thus permitting an analytical calculation of A_{vib} and U_{vib}. According to the Einstein model[19]

$$\omega_i = \omega_0, \qquad \Theta_E = \hbar\omega_0/k_B \tag{30}$$

In the Debye model, frequencies follow a parabolic distribution

$$f(\omega) = \frac{9N_h}{\omega^3_{max}}\omega^2, \qquad \Theta_D = \frac{\hbar\omega_{max}}{k_B} \tag{31}$$

$$0 < \omega < \omega_{max}$$

In the following the generic symbol Θ stands for Θ_E or Θ_D, for the Einstein and Debye model, respectively.

It is commonly assumed that the Grüneisen parameter [compare (10)]

$$\gamma = -\frac{\mathrm{d}\ln\Theta}{\mathrm{d}\ln V} \tag{32}$$

is independent of volume within the temperature range of interest. Both models lead to the Mie–Grüneisen equation of state, usually assumed to be of more general validity[19] than each of the distributions in (30) or (31):

$$P + \left.\frac{\partial U^{pot}_{min}}{\partial V}\right|_T = \gamma\frac{U_{vib}}{V} \tag{33}$$

Direct differentiation of (33), taking into account (10), (27), (30), (31), and (32), gives

$$B = \frac{1}{\kappa_T} = V\left.\frac{\partial^2 A}{\partial V^2}\right|_T = V\left.\frac{\partial^2 U^{pot}_{min}}{\partial V^2}\right|_T + \left.\frac{\partial U^{pot}_{min}}{\partial V}\right|_T + P - \frac{\gamma^2}{V}(TC_{vib} - U_{vib}) \tag{34}$$

where

$$C_{vib} = \left.\frac{\partial U_{vib}}{\partial T}\right|_V \simeq \rho_0 V c_\epsilon$$

From (28) and (33), the relative error in estimating $(\partial U/\partial V)|_T$ by $(\partial U^{pot}_{min}/\partial V)|_T$ is

$$\frac{\left.\frac{\partial U^{pot}_{min}}{\partial V}\right|_T - \left.\frac{\partial U}{\partial V}\right|_T}{\left.\frac{\partial U}{\partial V}\right|_T} = \frac{\left(\gamma\frac{U_{vib}}{V} - P\right) - \left(-P + \frac{\alpha_P}{\kappa_T}T\right)}{-P + \frac{\alpha_P}{\kappa_T}T} = \frac{\gamma\frac{U_{vib}}{V} - \gamma\frac{C_{vib}T}{V}}{-P + \frac{\gamma C_{vib}T}{V}}$$

and, for ordinary pressures, where P is much smaller than $\gamma C_{vib}T/V$

$$\frac{\left.\frac{\partial U^{pot}_{min}}{\partial V}\right|_T - \left.\frac{\partial U}{\partial V}\right|_T}{\left.\frac{\partial U}{\partial V}\right|_T} = \frac{U_{vib}}{C_{vib}T} - 1 \tag{35}$$

From (29) (after omission of the configurational entropy term), (33), and (34) the relative error in estimating B by $V(\partial^2 U^{pot}_{min}/\partial V^2)|_T$ is

$$\frac{V\left.\frac{\partial^2 U^{pot}_{min}}{\partial V^2}\right|_T - B}{B} = -\frac{\frac{\gamma}{V}U_{vib} - \frac{\gamma^2}{V}(TC_{vib} - U_{vib})}{B} = -\frac{\gamma^2 C_{vib}T}{VB}\left(\frac{1+\gamma}{\gamma}\frac{U_{vib}}{C_{vib}T} - 1\right) \tag{36}$$

Equations 35 and 36 permit direct numerical evaluation of the relative errors associated with neglecting vibrational contributions.

For glassy atactic polypropylene, experimental values at $T = 233$ K are (this is the temperature of interest in this paper, see also below)

$\alpha_P =$ 2.5×10^{-4} K^{-1} (p 244 of ref 20, ref 21, p 60 of ref 6)

$B = 3340$ MPa (p 267 of ref 6)

$\rho = 892$ kg/m^3 (p 244 of ref 20)

$c_\epsilon = 1320$ J/kgK (pp 86–89 of ref 6)

whence

$$\frac{C_{vib}}{V} = 1.177 \times 10^6 \frac{\mathrm{J}}{\mathrm{m^3K}}$$

$$\gamma = 0.71$$

For both models examined, the quantity $U_{vib}/C_{vib}T$ is a known function of $\tilde{T} = \Theta/T$. For the *Einstein model*

$$\frac{U_{vib}}{C_{vib}T} = \frac{e^{2\tilde{T}_E} - 1}{2\tilde{T}_E e^{\tilde{T}_E}}, \qquad \tilde{T}_E = \frac{\Theta_E}{T} \tag{37}$$

For the *Debye model*

$$\frac{U_{vib}}{C_{vib}T} = \frac{\frac{3\tilde{T}_D}{8} + D(\tilde{T}_D)}{4D(\tilde{T}_D) - \frac{3\tilde{T}_D}{e^{\tilde{T}_D} - 1}}, \qquad \tilde{T}_D = \frac{\Theta_D}{T} \tag{38}$$

(Values of the Debye function $D(x) = (3/x^3)\int_0^x z^3/(e^z - 1)\,dz$ are tabulated on p 998 of ref 22).

It remains to select appropriate values for Θ_E and Θ_D. Such values are obtained experimentally from low-temperature heat capacity data; according to Bondi (p 398 of ref 15) most molecular, and especially polymeric glasses, have a Θ_D of the order of 120 K. Simha, Roe, and Nanda[23] give experimental values of Θ_E and Θ_D for a variety of glassy amorphous polymers. In all cases the Debye temperature is lower than 120 K. Thus, selecting $\Theta_D = 120$ K and $\Theta_E \simeq (3/4)\Theta_D = 90$ K (a conservative estimate) and $T = 233$ K, $\tilde{T}_E = 0.386$ and $\tilde{T}_D = 0.515$, and by the use of the experimental values listed above, (35)–(38) give

Einstein model:

$$\frac{\left.\frac{\partial U^{pot}{}_{min}}{\partial V}\right|_T - \left.\frac{\partial U}{\partial V}\right|_T}{\left.\frac{\partial U}{\partial V}\right|_T} = 0.025$$

$$\frac{V\left.\frac{\partial^2 U^{pot}{}_{min}}{\partial V^2}\right|_T - B}{B} = -0.060$$

Debye model:

$$\frac{\left.\frac{\partial U^{pot}{}_{min}}{\partial V}\right|_T - \left.\frac{\partial U}{\partial V}\right|_T}{\left.\frac{\partial U}{\partial V}\right|_T} = 0.027$$

$$\frac{V\left.\frac{\partial^2 U^{pot}{}_{min}}{\partial V^2}\right|_T - B}{B} = -0.061$$

Thus, for the conditions addressed here, the vibrational contributions in (28) and (29) are at most of the order 2.5% and 6%, respectively. In the following we *neglect* the vibrational contributions.

Modeling of Deformations

The above thermodynamic analysis has permitted us to neglect entropic contributions, and thus to estimate derivatives of Helmholtz energy using the corresponding derivatives of the internal energy. The statistical mechanical analysis has justified the use of the total potential energy of the static structure in place of the internal energy. We thus replace (28) and (29) by much simpler forms:

$$\left.\frac{\partial U}{\partial \xi}\right|_T = \left.\frac{\partial U^{pot}{}_{min}}{\partial \xi}\right|_T$$

(estimation of internal pressure and stress) (39)

$$\left.\frac{\partial^2 A}{\partial \xi^2}\right|_T = \left.\frac{\partial^2 U^{pot}{}_{min}}{\partial \xi^2}\right|_T$$

(estimation of elastic coefficients) (40)

The considerations presented above, and the simplifications to which they lead, have been crucial in the development of a methodology for simulating structure[1] and for predicting mechanical properties. (See below.)

Our modeling of deformation rests on the following assumptions. (Assumptions A–D are essentially restatements of the assumptions introduced for the development of the undeformed structures.[1])

A. The model is static; i.e., it does not incorporate thermal motion. Temperature enters only indirectly through specification of the density in the undeformed state.

B. The glassy polymer is pictured in configuration space as an ensemble of mutually inaccessible states of microscopic liquid disorder. Estimates of the macroscopic properties are obtained by arithmetic averaging of the responses of individual microstates to deformation. Each undeformed microstructure and all deformed structures obtained from it satisfy the requirements of detailed mechanical equilibrium.

C. Bond lengths and bond angles are kept fixed. Molecular rearrangement upon deformation occurs exclusively through rotation around skeletal bonds ("Strophon assumption").

D. Backbone carbons and pendant hydrogen atoms are treated explicitly, whereas methyl groups are lumped into single "quasi-atom" entities.

E. Entropic contributions to the elastic coefficients are neglected; only potential energy effects are considered.

F. We concentrate on the elastic response to deformation. Viscoelastic phenomena associated with relaxation or flow are not considered. Thus we avoid chain slippage; i.e., each deformed microstate must be structurally similar to the undeformed microstate from which it is derived.

Assumptions A and B find justification in the thermodynamic and statistical mechanical considerations presented above. According to (39) and (40) the relevant quantity is the total potential energy, $U^{pot}{}_{min}$, of a local minimum in configuration space. It is the changes in this quantity that we have to monitor as a function of deformation in order to predict the mechanical properties. Assumption C follows directly from the analysis of the vibrational contributions associated with the hard degrees of freedom (see above). Assumption E is a consequence of the above thermodynamic analysis. Assumption F leads us to consider only very small degrees of deformation. According to a rule of thumb[17] polymer glasses are linearly elastic up to deformations of approximately 1%. We limit ourselves to deformations smaller than that. In general, our assumptions have been designed so as to give a model that is realistic, and at the same time, tractable with available computational resources.[1]

A frequently used assumption is that of "affine" or "homogeneous" (p 9 of ref 11) or "quasicontinuum" deformation, whereby all atom coordinates are transformed by a simple linear rule ($\mathbf{A}$ is a transformation matrix and $\mathbf{I}$ the unit matrix of order three)

$$\mathbf{r}^{affine} = \mathbf{A}\mathbf{r}_0 + \mathbf{b} \quad (41)$$

and (see eq 1)

$$\epsilon^{affine} = (1/2)(\mathbf{A}^T\mathbf{A} - \mathbf{I}) \simeq (1/2)(\mathbf{A}^T + \mathbf{A}) - \mathbf{I} \quad (42)$$

Such an affine transformation is impossible in our model systems because it would entail distortion of bond lengths and bond angles, contrary to the requirements of assumption C. Moreover, the structure resulting from an affine transformation will not, in general, satisfy the requirement of detailed mechanical equilibrium (assumption B). Thus, deformation in our bonded systems has to be introduced in a more subtle way.

The method we developed for simulating deformation consists of the following steps:

1. Start with an undeformed structure in detailed mechanical equilibrium. The continuation geometry in the undeformed state is cubic; i.e., the continuation vectors $\mathbf{a}_{x0}$, $\mathbf{a}_{y0}$, and $\mathbf{a}_{z0}$ are mutually perpendicular and equal in magnitude. The starting structure is a member of the

ensemble of 15 structures described earlier[1] and satisfies the condition

$$U^{pot}(\psi_0, \varphi_0; \mathbf{a}_{x0}, \mathbf{a}_{y0}, \mathbf{a}_{x0}) = \min \tag{43}$$

2. Choose the type of deformation to be imposed. Choose a small degree of deformation ϵ, such that $|\epsilon| \ll 1$.

3. Modify the location of the cube origin $\mathbf{0}$ and the continuation vectors $\mathbf{a}_x$, $\mathbf{a}_y$, and $\mathbf{a}_z$ so that they correspond to the chosen deformation. For the simple deformations studied here, initial system quantities ($\mathbf{0}_0$, $\mathbf{a}_{x0}$, $\mathbf{a}_{y0}$, $\mathbf{a}_{z0}$) are transformed to give the deformed system quantities ($\mathbf{0}$, $\mathbf{a}_x$, $\mathbf{a}_y$, $\mathbf{a}_z$) as follows.

uniform hydrostatic compression

$$\mathbf{0} = \mathbf{0}_0 + \frac{1-(1-\epsilon)^{1/3}}{2}\{\mathbf{a}_{x0} + \mathbf{a}_{y0} + \mathbf{a}_{z0}\}$$
$$\mathbf{a}_x = (1-\epsilon)^{1/3}\mathbf{a}_{x0} \qquad \mathbf{a}_y = (1-\epsilon)^{1/3}\mathbf{a}_{y0} \tag{44}$$
$$\mathbf{a}_z = (1-\epsilon)^{1/3}\mathbf{a}_{z0}$$

pure shear (perpendicular to z, along x)

$$\mathbf{0} = \mathbf{0}_0 - (1/2)\epsilon\mathbf{a}_{x0} \qquad \mathbf{a}_x = \mathbf{a}_{x0} \qquad \mathbf{a}_y = \mathbf{a}_{y0}$$
$$\mathbf{a}_z = \mathbf{a}_{z0} + \epsilon\mathbf{a}_{x0} \tag{45}$$

pure uniaxial tension (along x)

$$\mathbf{0} = \mathbf{0}_0 - (1/2)\epsilon\mathbf{a}_{x0} \qquad \mathbf{a}_x = (1+\epsilon)\mathbf{a}_{x0} \qquad \mathbf{a}_y = \mathbf{a}_{y0}$$
$$\mathbf{a}_z = \mathbf{a}_{z0} \tag{46}$$

In (44)–(46) $\mathbf{0}$ has been chosen in order to have the center of the cube remain unchanged during deformation. Other shear and tension deformations are obtained from (45) and (46) by cyclic permutation. The degrees of freedom of the undeformed system (ψ_0, φ_0), together with the continuation vectors $\mathbf{a}_x$, $\mathbf{a}_y$, $\mathbf{a}_z$, define a new initial guess structure, which is not in detailed mechanical equilibrium.

4. Starting from this initial guess structure, minimize the total potential energy with respect to the $2x + 1$ microscopic degrees of freedom (ψ, φ), keeping the continuation vectors equal to their deformed values:

$$U^{pot}(\psi, \varphi; \mathbf{a}_x, \mathbf{a}_y, \mathbf{a}_z) = \min \tag{47}$$

The resulting structure again satisfies the conditions of detailed mechanical equilibrium, but under the continuation geometry dictated by the mode and degree of deformation chosen in step 2 (compare eq 43 and 47); it is a "*deformed model structure*". The minimization (eq 47) is performed by using the BFGS quasi-Newton algorithm. Analytical expressions are used for the gradient with respect to the vector of unknowns ($\mathbf{r}_{C_0}$, ψ, φ). They are given in Appendix 1 of ref 1.

Computationally, the minimization problem (eq 47) is identical with the relaxation problem for the undeformed structure.[1] Since we want to realistically reproduce the elastic response of a glassy structure to small deformations, the "full" nonbonded interaction and torsional potential functions are used throughout the minimization.[1] Parameters have been described earlier.[1] The computation of U^{pot} requires solution of the minimum image problem in noncubic continuation geometries. We implement an efficient "screening" algorithm of our own construction,[25] which is applicable to both orthogonal and sheared systems. The computation time for an energy and gradient evaluation on the MIT Honeywell DPS 8/70 computer is 77 s.[1] Reaching a minimum energy deformed model structure typically requires 300–450 function evaluations.

5. To study different degrees of deformation, change ϵ and go back to step 3.

Step 4 in this procedure requires large amounts of computer time. We implemented a computational expedient, which consists of a preliminary "approximately affine" deformation. It was carried out between steps 3 and 4 as follows:

(3a) Bring the cube interior as close as possible to an affine deformation. This is done by minimizing the sum of squares of the differences between actual and affinely deformed coordinates.

$$\sum_{i=1}^{6x-1}\{\mathbf{r}_i(\mathbf{r}_{c0}, \psi, \varphi; \mathbf{a}_x, \mathbf{a}_y, \mathbf{a}_z) - \mathbf{r}_i^{affine}(\mathbf{r}_{0,i}, \mathbf{0}_0, \mathbf{a}_{x0}, \mathbf{a}_{y0}, \mathbf{a}_{z0}, \epsilon)\}^2 = \min \tag{48}$$

During this minimization the continuation vectors $\mathbf{a}_x$, $\mathbf{a}_y$, and $\mathbf{a}_z$ are fixed at their deformed values. Also, the continuation coefficients[1] of each atom are kept equal to their values in the undeformed state. Minimization is performed with respect to the $2x + 4 = 156$ variables ($\mathbf{r}_{C_0}$, ψ, φ) by using the undeformed state values ($\mathbf{r}_{C_0}$, ψ_0, φ_0) as initial guess. The constants $\mathbf{r}_i^{affine}$ for each type of deformation are determined as follows:

uniform hydrostatic compression

$$\mathbf{r}^{affine} = \mathbf{0}_0 + \frac{1-(1-\epsilon)^{1/3}}{2}\{\mathbf{a}_{x0} + \mathbf{a}_{y0} + \mathbf{a}_{z0}\} + (\mathbf{r}_0 - \mathbf{0}_0)(1-\epsilon)^{1/3} \tag{49}$$

pure shear (perpendicular to z, along x)

$$\mathbf{r}^{affine} = \mathbf{r}_0 + \epsilon\left\{\frac{(\mathbf{r}_0 - \mathbf{0}_0)\cdot(\mathbf{a}_{x0} \times \mathbf{a}_{y0})}{\mathbf{a}_{z0}\cdot(\mathbf{a}_{x0} \times \mathbf{a}_{y0})} - \frac{1}{2}\right\}\mathbf{a}_{x0} \tag{50}$$

pure uniaxial tension (along x)

$$\mathbf{r}^{affine} = \mathbf{r}_0 + \epsilon\left\{\frac{(\mathbf{r}_0 - \mathbf{0}_0)\cdot(\mathbf{a}_{y0} \times \mathbf{a}_{z0})}{\mathbf{a}_{x0}\cdot(\mathbf{a}_{y0} \times \mathbf{a}_{z0})} - \frac{1}{2}\right\}\mathbf{a}_{x0} \tag{51}$$

Equations 49, 50, and 51 are of the general form (eq 41). One can easily verify that they are the affine transformation equations corresponding to the changes in (44), (45), and (46) and that they leave the cube center unchanged. Affine equations for other shears and tensions are obtained from (50) and (51) by cyclic permutation Affine equations for other shears and tensions are obtained from (50) and (51) by cyclic permutation. Approximately 300 function and gradient evaluations are typically needed to reach the minimum. The CPU time per function and gradient evaluation at the MIT Honeywell DPS 8/70 is less than 2 s. The sum, over all 455 atoms, of the squared deviations from affine displacement at the minimum is typically about 0.5×10^{-3} Å^2 in the case of shear, about 0.1×10^{-2} Å^2 in the case of compression, and about 0.2×10^{-2} Å^2 in the case of uniaxial tension. Use of step 3a typically reduces the number of function evaluations in step 4 by ca. 100; it reduces the overall computing effort by roughly 30%.

It must be emphasized again that step 3a, that of approximately affine deformation, is merely a computational expedient. Its purpose is to bring the structure closer to the deformed minimum energy configuration. Its utility lies in the fact that the minimization in (48) is much less time consuming that the minimization in (47). If we omit step 3a, we obtain *the same* deformed model structure, but at greater expense in computer time.

An observation worth mentioning here is that if one starts from a deformed model structure (result of step 4

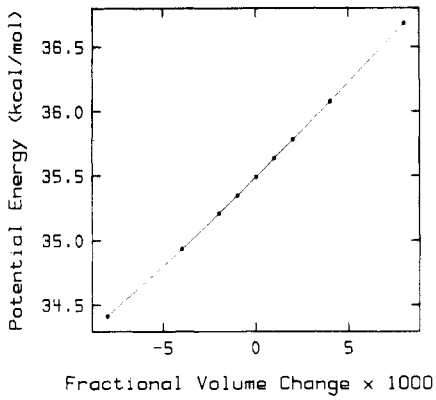

Figure 1. Total potential energy vs. fractional increase in volume for one model structure from hydrostatic compression–tension experiments. See text for details.

above) and reverses the deformation by changing the continuation vectors $\mathbf{a}_x$, $\mathbf{a}_y$, $\mathbf{a}_z$ back to $\mathbf{a}_{x0}$, $\mathbf{a}_{y0}$, $\mathbf{a}_{z0}$, and minimizes $U^{\text{pot}}(\psi, \varphi; \mathbf{a}_{x0}, \mathbf{a}_{y0}, \mathbf{a}_{z0})$, one reaches the original undeformed model structure (ψ_0, φ_0); within the strain range studied (ϵ of the order 10^{-3}) the model system's response to deformation is completely reversible (or "elastic"), as demanded by assumption F. The detailed mechanical equilibrium requirement $U^{\text{pot}}(\psi, \varphi; \epsilon) = \min$ seems to have a *unique* solution (ψ, φ) around the undeformed state (ψ_0, φ_0) within the range of degrees of deformation studied. This uniqueness characteristic may cease to hold for considerably larger values of ϵ; a bifurcation in the minimum potential energy trajectory in configuration space might indicate the onset of flow.

Steps 3 and 4 constitute a new, perfectly general algorithm for the deformation of any periodic model system, which is of wider applicability and more rigorous than previous approaches (compare Chapter 4 of ref 11). Deformation is modeled as a progressive change in the periodic continuation conditions, and changes in the interior of the cube come as a consequence of displacements in its surroundings. The unconstrained minimization requirement (eq 47) introduces no artificial external forces on the interior of the modeled infinite continuum. Our scheme is totally free of preconceived assumptions (such as affine deformation). In the case of a simple lattice, where all atoms are equivalent, the sequence of steps 3 and 4 would naturally lead to an affinely deformed state, and our method thus contains affine deformation as a special case.

Performing the loop over steps 3–5 in a sequence corresponding to different degrees of deformation yields a sequence of deformed structures. Such a sequence, obtained from hydrostatic compression–tension runs, is represented in Figure 1 by the total potential energy as a function of the fractional increase in volume. The point representative of the undeformed state lies in the center. On either side of it lie points corresponding to compressions of $\epsilon = \pm 0.001, \pm 0.002, \pm 0.004$, and ± 0.008. All nine points fall on a smooth curve. For the modeling of macroscopic mechanical properties we only require the slope and the curvature around the undeformed state; thus, we choose to confine ourselves to degrees of deformation of ± 0.001. These two points, together with the undeformed system point, provide all the information necessary. Each undeformed structure is subjected to the following deformations:

1. Uniform Hydrostatic Compression. $\epsilon = \pm 0.001$. The degree of deformation, ϵ, is defined as a fractional decrease in volume. From (1) and (49) the strain tensor for this deformation is $\epsilon = -(\epsilon/3)$ diag (1,1,1) and the vector of six strain components is

$$\epsilon = [-\epsilon/3 \quad -\epsilon/3 \quad -\epsilon/3 \quad 0 \quad 0 \quad 0]^T \tag{52}$$

2. Pure Shear. (a) Perpendicular to z, along x, $\epsilon = \pm 0.001$; (b) perpendicular to z, along y, $\epsilon = \pm 0.001$; (c) perpendicular to x, along y, $\epsilon = \pm 0.001$.

The degree of deformation, ϵ, is defined as a component of shear strain. For the zx-shear transformation, for instance, the strain tensor [(1),(50)] is

$$\epsilon = \begin{bmatrix} 0 & 0 & \epsilon/2 \\ 0 & 0 & 0 \\ \epsilon/2 & 0 & 0 \end{bmatrix}$$

and the vector of six strain components is

$$\epsilon = [0 \quad 0 \quad 0 \quad 0 \quad \epsilon \quad 0]^T \tag{53}$$

Some additional experiments were carried out in shear perpendicular to x and parallel to z in order to check for consistency. The properties of an xz-sheared minimum energy structure were found to be identical with those of the corresponding zx-sheared minimum energy structure, as expected.

3. Pure Uniaxial Tension. (a) along x, $\epsilon = \pm 0.001$; (b) along y, $\epsilon = \pm 0.001$; (c) along z, $\epsilon = \pm 0.001$.

The degree of deformation, ϵ, is defined as a tensile strain. For example, in uniaxial tension along x the strain tensor [(1),(51)] ϵ is $\epsilon = \text{diag}\ (\epsilon,0,0)$ and the vector of six strain components is

$$\epsilon = [\epsilon \quad 0 \quad 0 \quad 0 \quad 0 \quad 0]^T \tag{54}$$

Calculation of the Internal Stress and the Elastic Coefficients

A total of fifteen undeformed model structures have been created;[1] eight of them were deformed as described above. Hence, eight sets of structures, each consisting of one undeformed and fourteen deformed states, were obtained. For each such set of structures estimates of the mechanical properties were deduced by three methods. The description of these methods follows.

Energy Approach. Taylor expansion of the total potential energy $U^{\text{pot}}{}_{\text{min}}$ in the degree of deformation ϵ around the undeformed state yields [see (11), (14), (39), and (40)]

$$U^{\text{pot}}{}_{\text{min}} = U^{\text{pot}}{}_{\text{min},0} + V_0 \sum_{LM} [\tau_{LM} + \rho_0 c_\epsilon T \gamma_{LM}] \epsilon_{LM} + \frac{1}{2} V_0 \sum_{LMNK} \sum C_{LMNK} \epsilon_{LM} \epsilon_{NK} \tag{55}$$

where the tensor appearing in the second term is the "internal stress" (eq 12) and C_{LMNK} is an element of the fourth-order tensor of isothermal elastic coefficients. When (52), (53), and (54) are substituted for the strain tensor, (55) then reduces to special forms in "compact" notation, as shown in (56)–(58).

uniform hydrostatic compression

$$U^{\text{pot}}{}_{\text{min}} = U^{\text{pot}}{}_{\text{min},0} - V_0(1/3)\ \text{Tr}(\tau + \rho_0 c_\epsilon T \gamma)_0 \epsilon + (1/2) V_0 (C_{1111} + C_{1122} + C_{1133} + C_{2211} + C_{2222} + C_{2233} + C_{3311} + C_{3322} + C_{3333})(\epsilon/9) = U^{\text{pot}}{}_{\text{min},0} - V_0 \left(-P + \frac{\alpha_P T}{\kappa_T} \right)_0 \epsilon + (1/2) V_0 B \epsilon^2 \tag{56}$$

where

$$\frac{\partial U^{\text{pot}}{}_{\text{min}}}{\partial \epsilon} \equiv V_0 \left(-P + \frac{\alpha_P T}{\kappa_T} \right)_0$$

$$\frac{\partial^2 U^{\text{pot}}{}_{\text{min}}}{\partial \epsilon^2} \equiv V_0 B$$

pure shear (perpendicular to z, along x)

$$U^{pot}_{min} = U^{pot}_{min,0} + V_0[\tau_{13} + \tau_{31} + \rho_0 c_\epsilon T(\gamma_{13} + \gamma_{31})]\epsilon/2 + (1/2)V_0[C_{1313} + C_{1331} + C_{3113} + C_{3131}] = U^{pot}_{min,0} + V_0(\tau_5 + \rho_0 c_\epsilon T\gamma_5)\epsilon + (1/2)V_0 C_{55}\epsilon^2 \quad (57)$$

where

$$\frac{\partial U^{pot}_{min}}{\partial \epsilon} \equiv V_0(\tau_5 + \rho_0 c_\epsilon T\gamma_5)$$

$$\frac{\partial^2 U^{pot}_{min}}{\partial \epsilon^2} \equiv V_0 C_{55}$$

pure uniaxial tension (along x)

$$U^{pot}_{min} = U^{pot}_{min,0} + V_0(\tau_{11} + \rho_0 c_\epsilon T\gamma_{11})\epsilon + (1/2)V_0 C_{1111}\epsilon^2 = U^{pot}_{min,0} + V_0(\tau_1 + \rho_0 c_\epsilon T\gamma_1)_0\epsilon + (1/2)V_0 C_{11}\epsilon^2 \quad (58)$$

where

$$\frac{\partial U^{pot}_{min}}{\partial \epsilon} \equiv V_0(\tau_1 + \rho_0 c_\epsilon T\gamma_1)_0$$

$$\frac{\partial^2 U^{pot}_{min}}{\partial \epsilon^2} \equiv V_0 C_{11}$$

The slopes and curvatures of $U^{pot}_{min,0}$ were estimated from the results of our deformation simulations by three-point finite-difference formulas. Contributions from long-range nonbonded interactions ("potential tails") are taken into account for compression and tension, since these do not conserve volume. The tail contribution is inversely proportional to system volume and has the form[1]

$$\Delta U^{pot}_{tails} = \Delta U_{tails,0}\left(\frac{V_0}{V}\right) \quad (59)$$

where in our case $\Delta U^{pot}_{tails,0} = -84.76$ kcal/(mol structures).

A test for internal consistency is provided by the fact that the "internal pressure", $-P + \alpha_p T/\kappa_T$, from (56) must be identical with $(1/3)\sum_{i=1}^{3}(\tau_i + \rho_0 c_\epsilon T\gamma_i) = (1/3)\mathrm{Tr}\sigma_0$, obtained from (58) and the two equivalent forms for tension along y and z. In our calculations they were always found to be equal.

In summary, the first derivatives in the *energy approach* lead (in the case of compression) to the internal pressure, $(-P + \alpha_p T/\kappa_T)_0$, and (in the case of shear and tension) to the internal stress tensor, σ_0 (all first derivative information pertains to the *undeformed state only*). From the second derivatives we obtain (in the case of compression) the bulk modulus B and (in the case of shear and tension) the *diagonal elements* of the 6×6 matrix of isothermal elastic coefficients, $\mathbf{C}$.

Force Approach. We proceed to solve the detailed force and torque balance equations for all atoms and bonds of each structure. According to our assumptions C and D above, and to our choice of potentials,[1] bonds are rigid sticks that exert on the atoms attached to them (i) forces of any magnitude and direction; (ii) torques of any magnitude in directions perpendicular to their axes; (iii) torques along their axes whose magnitude is defined by the intrinsic torsional potential function. (This refers to skeletal bonds which, although rigid and rigidly attached to the atoms they connect, can yield to rotation around their axis.)

Thus, atoms in our system experience the following (shown schematically in Figure 2):

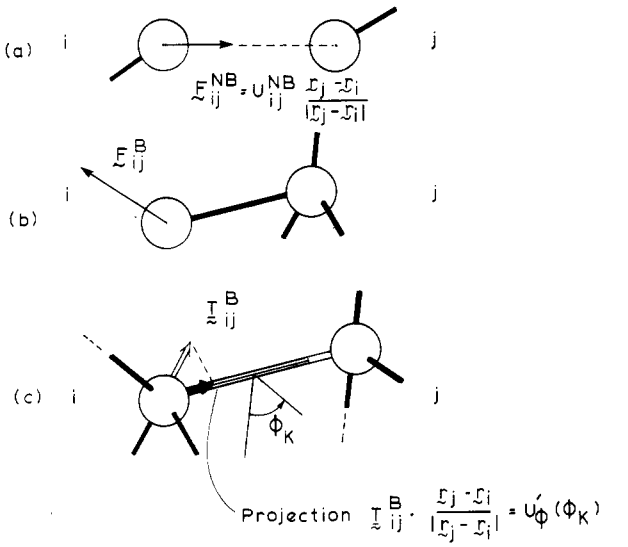

Figure 2. Interatomic forces and torques: (a) nonbonded forces; (b) bonded forces; (c) bonded torques.

(a) Nonbonded Forces. These are central and dictated by the nonbonded interaction potential. The nonbonded force on atom i, due to atom j, is

$$\mathbf{F}^{NB}_{ij} = \left.\frac{dU^{NB}_{ij}}{dr}\right|_{r=|\mathbf{r}_i-\mathbf{r}_j|} \frac{\mathbf{r}_j - \mathbf{r}_i}{|\mathbf{r}_j - \mathbf{r}_i|} \quad (60)$$

One need not consider nonbonded forces between atom pairs whose separation is fixed by connectivity.[1]

(b) Bonded Forces. These are, in general, noncentral. Their magnitude and direction are determined by the balance condition (see below). The bonded force exerted at atom i from atom j through bond ij is $\mathbf{F}^{B}_{ij}$.

(c) Bonded Torques. These are exerted on skeletal carbons through either pendant or skeletal bonds. Their magnitude and direction are determined by the balance conditions. $\boldsymbol{T}^{B}_{ij}$ is the torque exerted on atom i by atom j through the bond ij. If the bond is skeletal, characterized by a torsion (dihedral) angle φ_k, the component of the torque $\boldsymbol{T}^{B}_{ij}$ that is exerted along the axis of the bond is dictated by the intrinsic torsional potential function:

$$\boldsymbol{T}^{B}_{ij} \cdot \frac{\mathbf{r}_j - \mathbf{r}_i}{|\mathbf{r}_j - \mathbf{r}_i|} = \left.\frac{dU_\varphi}{d\varphi}\right|_{\varphi=\varphi_k} \quad (61)$$

The requirement of detailed mechanical equilibrium demands that

$$\sum \mathbf{F} = \mathbf{0}, \qquad \sum \boldsymbol{T} = \mathbf{0} \qquad \text{for all atoms, all bonds} \quad (62)$$

The set of detailed force and torque balances (eq 62) is equivalent to the requirement (eq 47) of minimum potential energy. The static undeformed and deformed structures constitute solutions to the set of (62). The values of the microscopic degrees of freedom (ψ, φ) have been specified through the minimization (eq 51), and the set of (62) is overdetermined. Thus, $(2x + 1) = 153$ consistency checks can be carried out per structure, and the accuracy of the minimizations can be checked.

The balances (62) were solved in a segment-by-segment fashion "along" a parent chain, and the forces and torques exerted on each atom and each bond of each structure were computed. The explicit form of (62) as well as the solution procedure are described in Appendix B. It was found that in all (undeformed and deformed) systems the balances close with a relative error of less than 10^{-5} (see Appendix B).

From the atomic forces and torques the total forces $\mathbf{F}_f$ exerted on the interior of the model "box" by its sur-

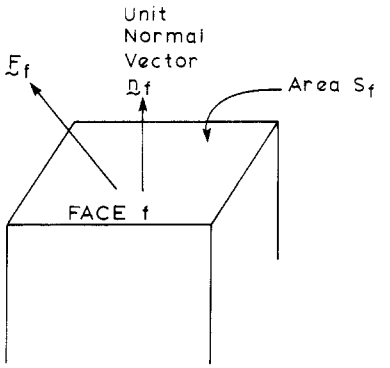

Figure 3. Face forces $\mathbf{F}_f$, face area S_f, and face normal $\mathbf{n}_f$.

roundings through each of its faces can be obtained. This is done by summing individual forces (bonded *and* nonbonded) and torques exerted on "interior" atoms from surrounding atoms through each face. In a periodic system such as ours "face forces" $\mathbf{F}_f$ exerted on opposite faces of the box must be such that their sum is 0. The internal stress tensor σ (see eq 12) is related to the face forces $\mathbf{F}_f$ through (compare eq 2)

$$\mathbf{F}_f = \sigma^T \mathbf{n}_f S_f \tag{63}$$

where $\mathbf{n}_f$ is the unit normal vector perpendicular to face f and S_f the area of face f, as indicated in Figure 3. Solving the nine independent eq 63 for the nine elements of σ yields a tensor that is symmetric to an excellent approximation; this is an additional indication of closure of the balance equations.

Thus, from the *force approach* one obtains, by *direct* calculation, the internal stress tensor σ in the *undeformed and in all deformed states.* (Note that the calculation of the undeformed stress tensor σ_0 requires no information from the deformed states, unlike the corresponding calculation with the *energy approach.*) Furthermore, (55) indicates that the isothermal elastic coefficients can be obtained from the first derivatives of the components of the internal stress with respect to strain. Hence, one can calculate the *full* 6 × 6 matrix **C** of elastic coefficients from the slopes $\partial\sigma_{LM}/\partial\epsilon$ in tension and shear. A single tension experiment provides one of the first three columns of the **C** matrix; a single shear experiment provides one of the last three columns. Since we perform a pair of computer experiments in each mode of deformation ($\epsilon = \pm 0.001$), we have two estimates for each element of the **C** matrix. These estimates, as a rule, agree very well with each other, indicating that changes upon deformation are symmetric around the undeformed state (*harmonic behavior*). Theoretical estimates of the **C** matrix are to a very good approximation symmetric, which constitutes an additional confirmation of consistency.

In summary, the *force approach* yields more information than the *energy* approach because it is much more detailed. Those quantities (σ_0 and the diagonal elements of **C**) that can be obtained by both approaches are found to be practically identical, as is theoretically expected.

Virial Theorem. The virial theorem approach constitutes an alternative formulation of the *force approach.* The virial theorem of statistical mechanics[26] gives the stress tensor τ in a macroscopic, bounded system in terms of the atomic momentums $\mathbf{p}_i$, masses m_i, coordinates $\mathbf{r}_i$, and interatomic forces $\mathbf{F}_{ij}$ as

$$\tau_{LM} = -\frac{1}{V}\left\langle \sum_i \frac{p_{i,L}p_{i,M}}{m_i} \right\rangle - \frac{1}{2V}\left\langle \sum_i \sum_{j\neq i} (r_{i,L} - r_{j,L})F_{ij,M} \right\rangle \tag{64}$$

(Brackets denote ensemble averages). In a static, unbounded, periodic model structure the appropriate form of (64) can be shown to be

$$\sigma_{LM} = -\frac{1}{2V}\left\{ \sum_i \sum_{j\neq i} (r_{i,L} - r_{j,L})_{\min} F^{\min}{}_{ij,M} \right\} \tag{65}$$

where min denotes distances and forces between minimum-image (hence interacting) pairs of atoms. Both bonded and nonbonded forces are included in F_{ij}, i.e.

$$\mathbf{F}_{ij} = \mathbf{F}^{\mathrm{B}}{}_{ij} + \mathbf{F}^{\mathrm{NB}}{}_{ij} \tag{66}$$

Equation 65 provides a means of directly calculating the internal stress tensor from interatomic forces, which are computed from the detailed force and torque balances as discussed in Appendix B. Since only minimum-image pairs are involved, it is evident that σ is invariant to translations of the chain origin.

The σ tensor obtained by applying (65) to each of the undeformed and deformed structures is identical to the one obtained by the *force approach* described above. Results are treated in the same way to arrive at estimates of the elastic coefficients. The actual equivalence between the *force approach* and the *virial theorem approach* is proved in Appendix C.

Results

Elastic Constants. Average values and standard deviations of the diagonal elastic coefficients and of the bulk modulus, obtained by the *energy approach* from the eight structures studied in deformation, are listed below.

$$\mathbf{C} = \begin{bmatrix} 4777 \pm 497 & & & & & \\ & 5871 \pm 774 & & & & \\ & & 3507 \pm 495 & & & \\ & & & 896 \pm 439 & & \\ & & & & 1230 \pm 136 & \\ & & & & & 1230 \pm 326 \end{bmatrix} \text{MPa} \tag{67}$$

$$B = 3270 \pm 415 \text{ MPa} \tag{68}$$

Our estimate of the 6 × 6 matrix of elastic coefficients from the *force (or virial theorem) approach* is presented in (69), in the same form. The diagonal elements of (69) are in excellent agreement with (67). For a macroscopic, isotropic material the **C** matrix (eq 69) should assume the form of (7). The small size of the model systems, however, induces considerable fluctuations of the properties in different directions within a given structure. In addition there are fluctuations from structure to structure for the same property in a given direction. Nevertheless, it is obvious that the nonzero elements of (7) are dominant in (69) and that all elements deviate from the values suggested by (7) by less than two standard deviations.

$$\mathbf{C} = \begin{bmatrix} 4773 \pm 498 & 3244 \pm 542 & 2047 \pm 355 & 93 \pm 242 & -243 \pm 274 & 51 \pm 231 \\ 3244 \pm 542 & 5871 \pm 772 & 2943 \pm 557 & 777 \pm 707 & -162 \pm 167 & 502 \pm 384 \\ 2047 \pm 355 & 2943 \pm 557 & 3492 \pm 497 & 695 \pm 497 & -367 \pm 191 & -31 \pm 158 \\ 93 \pm 242 & 777 \pm 707 & 695 \pm 497 & 858 \pm 472 & 8 \pm 64 & -696 \pm 477 \\ -243 \pm 274 & -162 \pm 167 & -367 \pm 191 & 8 \pm 64 & 1230 \pm 135 & 176 \pm 179 \\ 51 \pm 231 & 502 \pm 384 & -31 \pm 158 & -696 \pm 477 & 176 \pm 179 & 1221 \pm 333 \end{bmatrix} \text{MPa} \tag{69}$$

Table I
Comparison of Experimental and Predicted Values of the Elastic Constants

		theory			
		energy approach		force approach	
property	exptl value[a]	value	deviation from expt, %	value	deviation from expt, %
Lamé const, λ, MPa	2690	2520	−6.3	2700	+0.4
Lamé const, μ, MPa	970	1110	+14.4	1020	+5.2
G, MPa	970	1110	+14.3	1020	+5.2
E, MPa	2650	2990	+12.8	2790	+5.3
B, MPa	3340	3250	−2.6	3390	+1.5
ν	0.37	0.35	−5.4	0.36	−2.7

[a] References 6 and 28; see text for details.

To obtain estimates of the elastic constants for comparison with experiments we proceed as follows.

Energy approach. We average tension and shear results over all structures and over all directions. Mean values and standard deviations of the means thus obtained are listed below. Observe that each value comes from 24 independent contributions, whereas each entry of (67) represented an average of 8 numbers. Also, the estimate of B from hydrostatic compression [compare (68)] is given, in which directional averaging is implicit.

(tension)

$$(1/3)(C_{11} + C_{22} + C_{33}) = 4718 \pm 389 \text{ MPa} = 2\mu + \lambda \tag{70a}$$

(shear)

$$(1/3)(C_{44} + C_{55} + C_{66}) = 1119 \pm 182 \text{ MPa} = \mu \tag{70b}$$

(compression)

$$B = 3270 \pm 415 \text{ MPa} = \lambda + (2/3)\mu \tag{70c}$$

Equations 7 and 8 impose simple relationships on the values listed in eq 70. The Lamé constants λ and μ can be obtained from any two of the three entries in (70), and checking against the third confirms that the three model estimates are consistent within 1%. Thus, the model ensemble's response to small deformations conforms to that of an isotropic elastic solid.

The values of λ and μ that best describe the results (eq 70), together with the values of the elastic constants obtained through (8), are listed in the third column of Table I.

Force Approach. Averaging the estimates of the elastic coefficients from the *force* approach over all structures and all orientations (compare (69)), we obtain

(tension)

$$(1/3)(C_{11} + C_{22} + C_{33}) = 4712 \pm 390 \text{ MPa} = 2\mu + \lambda \tag{71a}$$

(tension)

$$(1/3)(C_{12} + C_{23} + C_{31}) = 2745 \pm 292 \text{ MPa} = \lambda \tag{71b}$$

(shear)

$$(1/3)(C_{44} + C_{55} + C_{66}) = 1103 \pm 192 \text{ MPa} = \mu \tag{71c}$$

The three values in (71) are consistent in λ and μ within 5%. The best values of λ and μ that describe the results, together with the elastic constants obtained through (8), are listed in the fifth column of Table I.

Comparison of Theory with Experiment. Experimental data on the mechanical properties of glassy *atactic* polypropylene are relatively rare. Direct measurements of the Young's modulus of elasticity, E, on atactic polypropylene in the glassy region have been performed by Sauer et al.;[28] at −40 °C, by mechanical testing at audio frequencies on samples of molecular weight of 3×10^5 and 0% crystallinity, they find

$$\text{experiment: } E = 2560 \text{ MPa} \tag{72}$$

An experimental value of $B = 3500$ MPa for the bulk modulus is reported (p 27 of ref 6), but it probably refers to the isotactic, semicrystalline form of the polymer and to room temperature. A better value is obtained from the correlation presented on p 267 of ref 6: for atactic polypropylene at −40 °C, a bulk modulus of

$$\text{experiment: } B = 3340 \text{ MPa} \tag{73}$$

is most plausible. Values of (72) and (73), together with the constants λ, μ, G, and ν obtained from them, are listed in the first column of Table I. Observe that G is very close to the typical "glassy" value of 1000 MPa and that ν obeys the rule of thumb that "all glassy polymers have a Poisson ratio of approximately 1/3" (p 111 of ref 13). The experimental values listed in Table I are though to be accurate to within 15%.

Relative deviations between the theoretical estimates and the corresponding experimental values are listed in the fourth and sixth columns of Table I for the energy and the force approach, respectively. One must reiterate here that the model has *no adjustable parameters*. Also, there is an uncertainty associated with the theoretical values, an estimate of which is provided by the standard deviations in (70) and (71). The *energy approach* predicts all elastic constants with a relative error of less than 15%. Estimates obtained by the *force approach* are in even better agreement with experiment. We can conclude that our methods are remarkably successful in estimating elastic constants.

Thermal Expansion Coefficient. The ensemble-averaged internal stress tensor in the undeformed state, σ_0, obtained from the 15 model structures by the force approach, assumes the form (mean values ± standard deviations of the mean)

$$\sigma_0 = \begin{bmatrix} 82.4 \pm 26.6 & -17.9 \pm 12.4 & -0.2 \pm 12.3 \\ -17.9 \pm 12.4 & 67.3 \pm 40.2 & -7.2 \pm 11.0 \\ -0.2 \pm 12.3 & -7.2 \pm 11.0 & 96.9 \pm 22.9 \end{bmatrix} \text{MPa} \tag{74}$$

Within the framework of this static model it is not possible to separate the external stress contribution (τ_0) from the Grüneisen tensor contribution ($\rho_0 c_\epsilon T \gamma_0$) to the internal stress tensor σ_0. For ordinary external loads, however (an external pressure of 1 atm has been assumed in specifying the density of the undeformed system[1]), the Grüneisen tensor contribution, which is a measure of cohesive forces in the polymeric solid, is clearly dominant. For an isotropic, macroscopic material σ_0 must then be diagonal, with all diagonal elements equal (compare eq 10). The model estimates (eq 74) do not strictly satisfy this requirement because of limited sample size, but all off-diagonal elements are 0 within two standard deviations, and the diagonal elements are equal within the same limits.

The trace of σ_0 can be used to estimate the ratio of the thermal expansion coefficient to compressibility:

$$\frac{\alpha_P}{\kappa_T} = \frac{1}{3T} \text{Tr}(\sigma_0) + \frac{P}{T} \tag{75}$$

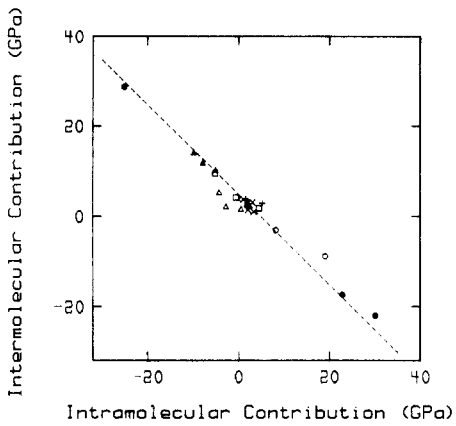

Figure 4. Inter- and intramolecular contributions to the three first diagonal elements of the 6 × 6 matrix of isothermal elastic coefficients. See text for details.

Using P = 1 atm and T = 223 K, we obtain α_P/κ_T = 0.35 ± 0.06 MPa/K.

With the calculated value for the bulk modulus (eq 68) a theoretical estimate of the thermal expansion coefficient is

$$\alpha_P = (1.08 \pm 0.23) \times 10^{-4}\ \mathrm{K}^{-1} \qquad (76)$$

Zakin et al.[21] have carried out measurements of the thermal expansion of an isotactic polypropylene (18% crystalline). Their value for −40 °C is 2.51 × 10^{-4} K^{-1}. An experimental curve of specific volume vs. temperature for atactic polypropylene is given on p 294 of ref 20. From it the thermal expanion coefficient of the glassy atactic polymer at −40 °C is 2.7 × 10^{-4} K^{-1}. Experimental values given on p 60 of ref 6, in contrast, lead to a value of 2.0 × 10^{-4} K^{-1}. We accept here as representative value

$$\text{experiment: } \alpha_P = 2.5 \times 10^{-4}\ \mathrm{K}^{-1} \qquad (77)$$

The theoretical estimate (eq 76) is too low by a factor of 2.5. An analysis of the sensitivity of the computer estimates to perturbations in the potential parameters used show that the estimate of the thermal expansion coefficient, unlike those of the elastic constants and the solubility parameter, can change significantly with small changes in the potential energy parameters (see Appendix D); e.g., a slightly inappropriate choice of the van der Waals radii may be responsible for the discrepancy between (76) and (77).

Intra- vs. Intermolecular Contributions to Elastic Response. Following Yannas and Luise,[8] we now separate between intramolecular and intermolecular contributions to the elastic response. *Intramolecular* contributions to σ_0 and **C** are computed from changes in the parent-chain energy with deformation. Equations 56–58 are used, but $U^{\mathrm{pot}}_{\mathrm{min}}$ is replaced by the total potential energy of an isolated parent chain, computed with the "full" Lennard-Jones potenial function. *Intermolecular* contributions are determined as the difference between the intramolecular quantities and the appropriate total. They, too, can be regarded as being determined by (56–58) if $U^{\mathrm{pot}}_{\mathrm{min}}$ is replaced by the cohesive energy of a structure.[1]

Inter- vs. intramolecular contributions to the three first diagonal elements of the **C** matrix (C_{11}, C_{22}, and C_{33}), obtained from the eight structures that were deformed, are plotted in Figure 4. There is a total of 24 points. Each point comes from a pair of uniaxial tension "experiments". Points from the same structure have been plotted with the same symbol. The broken line corresponds to the equation (compare Table I)

$$C_{II}^{\mathrm{inter}} + C_{II}^{\mathrm{intra}} = 2\mu + \lambda = 4740\ \mathrm{MPa},\ I = 1, 2, 3 \qquad (78)$$

One clearly observes a strong negative correlation between the inter- and intramolecular contributions to the C_{II}'s. Each of these contributions may vary widely, but their sum is approximately constant. The same conclusion is reached by comparing inter- and intramolecular shear moduli, or compressibility. The wide variation in the intramolecular elastic coefficients probably reflects the high multiplicity of single chain conformations within the polymer. The intermolecular interactions between different chains strongly dampen the effects of individual chain idiosyncrasy, however. The relationship between inter- and intramolecular contributions is therefore *not* synergistic, but antagonistic.

The intramolecular part of the internal stress tensor, averaged over the eight deformed structures assumes the form

$$\sigma_{\mathrm{intra}} = \begin{bmatrix} -146.7 \pm 38.5 & 11.2 \pm 24.0 & 11.2 \pm 11.0 \\ 11.2 \pm 24.0 & -203.8 \pm 57.6 & 32.4 \pm 46.9 \\ 11.2 \pm 11.0 & 32.4 \pm 46.9 & -150.4 \pm 29.8 \end{bmatrix} \mathrm{MPa} \qquad (79)$$

All diagonal elements in this intramolecular tensor are *negative*, in marked contrast to those of the total tensor (eq 74). (The energy of an isolated parent chain would decrease if the chain were allowed to expand.) In other words, single chains in the polymer are under compression by their neighbors. Coexistence in the bulk requires suppression of the tendency of individual chains to expand due to "excluded volume" effects. This, of course, is merely a restatement of Flory's "random coil hypothesis" (p 602 of ref 29).

Microscopic vs. Macroscopic Stability

As we mentioned earlier,[1] the fact that each of the microstructures is in detailed mechanical equilibrium does not imply that our model glass is in stable thermodynamic equilibrium. Here we further elucidate this distinction, using the deformation results.

The condition for stable *mechanical equilibrium* in a microscopic structure is[1]

$$\mathbf{H}\text{: positive definite} \qquad (80)$$

where **H** is the Hessian matrix of the total potential energy with respect to the microscopic degrees of freedom. The *thermodynamic criterion of stability* for an elastic solid is (Chapter 13 of ref 12)

$$\mathbf{C}\text{: positive definite} \qquad (81)$$

where **C** is the 6 × 6 matrix of isothermal elastic coefficients. All our model structures satisfy the microscopic criterion 80, by construction. However, application of the thermodynamic criterion (eq 81) to the individual microstructures led to the conclusion that two of the eight structures studied in deformation are not stable thermodynamically. For these structures modes of deformation exist in which the total energy is *concave* with respect to an externally imposed macroscopic strain. Our model deformations thus provide direct proof of the fact that criteria 80 and 81 need not be simultaneously fulfilled. Although the ensemble-averaged matrix **C** (eq 69) is positive definite, the existence of microstructures whose response to deformation does not satisfy criterion 81 may shed some light on the inherent "instability" of real

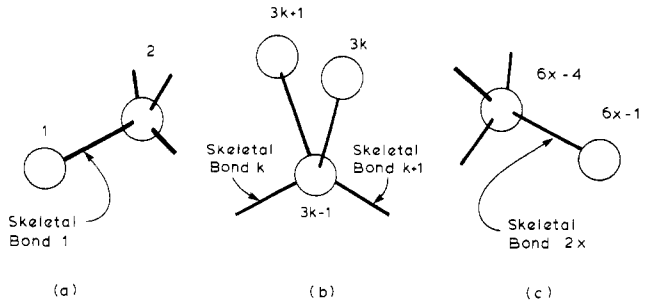

Figure 5. Notation for the solution of detailed force and torque balance equations: (a) first segment; (b) intermediate segment; (c) last segment.

Table II
van der Waals Radii, in Å

species	H	C	R
I. base case	1.3	1.8	2.0
II. perturbed case	1.2	1.7	2.0

Table III
Changes in Estimated Properties

property	I, value, base case	II, value, perturbed case	change, %
solubility parameter δ, $(J/cm^3)^{1/2}$	14.6	15.6	+6.8
$^1/_3(C_{11} + C_{22} + C_{33})$, MPa	6524	5303	-18.7
$^1/_3(C_{44} + C_{55} + C_{66})$, MPa	1278	1337	+4.6
α_P/κ_T, MPa/K	-0.175	+0.717	-509.7

polymeric glasses.

Acknowledgment. We gratefully acknowledge support from the National Science Foundation (Polymer Program) under Grant No. DMR-8312694 and Amendment No. 01 (Class VI Computing Services) and the Texaco–Mangelsdorf Associate Professorship at the Massachusetts Institute of Technology. We also thank Professors A. S. Argon, R. E. Cohen, and I. V. Yannas for invigorating discussions.

Appendix A: Criterion for the Significance of Entropic Effects in Elastic Deformation

We will derive criterion 15 from the less useful form (eq 14). For an arbitrary thermodynamic quantity a, characteristic of an elastic solid, we may write

$$a = a(T, \tau) = a(T, \tau\,(T,\epsilon)) \tag{A.1}$$

Then

$$\left.\frac{\partial a}{\partial T}\right|_\epsilon = \left.\frac{\partial a}{\partial T}\right|_\tau + \sum_{LM}\left[\left.\frac{\partial a}{\partial \tau_{LM}}\right|_{T,\tau_{(LM)}} \left.\frac{\partial \tau_{LM}}{\partial T}\right|_\epsilon\right] \tag{A.2}$$

Considering $\tau = \tau(T, \epsilon)$ we have

$$d\tau_{LM} = \left.\frac{\partial \tau_{LM}}{\partial T}\right|_\epsilon dT + \sum_{NK} \frac{\partial \tau_{LM}}{\partial \epsilon_{NK}} d\epsilon_{NK}$$

hence

$$\left.\frac{\partial \tau_{LM}}{\partial T}\right|_\epsilon = -\sum_{NK} \frac{\partial \tau_{LM}}{\partial \epsilon_{NK}} \left.\frac{\partial \epsilon_{NK}}{\partial T}\right|_\tau = -\sum_{NK} C_{LMNK}\alpha_{NK} \tag{A.3}$$

where $\alpha = (\partial\epsilon/\partial T)|_\tau$ is the thermal expansion tensor (p 33 of ref 11). Combining (A.1) and (A.3)

$$\left.\frac{\partial a}{\partial T}\right|_\epsilon = \left.\frac{\partial a}{\partial T}\right|_\tau - \sum_{LM}\sum_{NK} C_{LMNK}\alpha_{NK} \left.\frac{\partial a}{\partial \tau_{LM}}\right|_{T,\tau_{(LM)}} \tag{A.4}$$

For an *isotropic solid*, we have $\alpha_{NK} = (\alpha_P/3)\delta_{NK}$, and (A.4) gives

$$\left.\frac{\partial a}{\partial T}\right|_\epsilon = \left.\frac{\partial a}{\partial T}\right|_\tau - \alpha_P \sum_{LM} \frac{C_{LM11} + C_{LM22} + C_{LM33}}{3} \left.\frac{\partial a}{\partial \tau_{LM}}\right|_{T,\tau_{(LM)}} \tag{A.5}$$

Furthermore, expressing all isothermal elastic coefficients as functions of the Lamé constants (eq 7) we obtain

$$\left.\frac{\partial a}{\partial T}\right|_\epsilon = \left.\frac{\partial a}{\partial T}\right|_\tau - \alpha_P\left(\lambda + \frac{2}{3}\mu\right)\left\{\left.\frac{\partial a}{\partial \tau_{11}}\right|_{T,\tau_{(11)}} + \left.\frac{\partial a}{\partial \tau_{22}}\right|_{T,\tau_{(22)}} + \left.\frac{\partial a}{\partial \tau_{33}}\right|_{T,\tau_{(33)}}\right\} \tag{A.6}$$

If we assume in addition to the isotropy of the system, that the distribution of stress is isotropic, all three derivatives within the curly brackets are equal. Application of the differential stresses $d\tau_{11}$, $d\tau_{22}$, and $d\tau_{33}$ on the system leads to a change in a equal to

$$da|_T = \left.\frac{\partial a}{\partial \tau_{11}}\right|_{T,\tau_{(11)}} d\tau_{11} + \left.\frac{\partial a}{\partial \tau_{22}}\right|_{T,\tau_{(22)}} d\tau_{22} + \left.\frac{\partial a}{\partial \tau_{33}}\right|_{T,\tau_{(33)}} d\tau_{33}$$
$$= \left.\frac{\partial a}{\partial \tau_{11}}\right|_{T,\tau_{(11)}} (d\tau_{11} + d\tau_{22} + d\tau_{33}) = -3\left.\frac{\partial a}{\partial \tau_{11}}\right|_{T,\tau_{(11)}} dP$$

whence

$$\left.\frac{\partial a}{\partial \tau_{11}}\right|_{T,\tau_{(11)}} = \left.\frac{\partial a}{\partial \tau_{22}}\right|_{T,\tau_{(22)}} = \left.\frac{\partial a}{\partial \tau_{33}}\right|_{T,\tau_{(33)}} = -\frac{1}{3}\left.\frac{\partial a}{\partial P}\right|_T \tag{A.7}$$

Therefore, by the use of (A.7) and (8), (A.6) becomes

$$\left.\frac{\partial a}{\partial T}\right|_\epsilon = \left.\frac{\partial a}{\partial T}\right|_P + \frac{\alpha_P}{\kappa_T}\left.\frac{\partial a}{\partial P}\right|_T \tag{A.8}$$

Application of (A.8) for $a = C_{LMNK}$ leads directly from criterion 14 to criterion 15.

Appendix B: Force and Torque Balance Equations

Consider a parent chain, CH_3–CHR–$(CH_2$–CHR$)_{x-1}$–CH_3, immersed in a sea of its neighbors. Following Flory[30] we number its skeletal bonds from 1 to $2x$ and its skeletal atoms from 0 to $2x$. Furthermore, we number its atoms from 1 to $6x - 1$ as follows (compare Figure 5): atoms 1 and $6x - 1$ are the terminal CH_3 substituents; atoms $3k - 1$, $1 \le k \le 2x - 1$ are skeletal carbons; they are chiral if k is odd and achiral if k is even; atoms $3k$, $1 \le k \le 2x - 1$ are pendant hydrogens; and atoms $3k + 1$, $1 \le k \le 2x - 1$ are pendant hydrogens (if k is even) or R substituents (if k is odd). We call "skeletal segment" a skeletal atom and all its substituents. Skeletal segment 0 consists of the terminal atom 1. Skeletal segment $2x$ consists of the terminal atom $6x - 1$. Skeletal segment k ($1 \le k \le 2x - 1$) consists of the carbon $3k - 1$ and the substituents $3k$ and $3k + 1$. Bond k connects skeletal segments $k - 1$ and k.

With the nomenclature, and with the notation introduced in the discussion of the force approach in the main text, the detailed force and torque balance equations assume the form:

Segment 0

Force balance on atom 1:

$$\mathbf{F}^B{}_{12} = \sum_{j\neq 1} \mathbf{F}^{NB}{}_{1j} \tag{B.1}$$

Torque balance on atom 1:

$$\boldsymbol{T}^B{}_{12} = \mathbf{0} \tag{B.2}$$

Force balance on bond 1:

$$(-\mathbf{F}^{B}_{12}) + (-\mathbf{F}^{B}_{21}) = \mathbf{0} \text{ and } \mathbf{F}^{B}_{21} = -\mathbf{F}^{B}_{12} \quad (B.3)$$

Torque balance on bond 1:

$$(-\boldsymbol{T}^{B}_{12}) + (\mathbf{r}_1 - \mathbf{r}_2) \times (-\mathbf{F}^{B}_{12}) + (\boldsymbol{T}^{B}_{21}) = 0$$

or

$$\boldsymbol{T}^{B}_{21} = \boldsymbol{T}^{B}_{12} - (\mathbf{r}_1 - \mathbf{r}_2) \times \mathbf{F}^{B}_{12} \quad (B.4)$$

Segment k, 1 ≤ k ≤ 2x - 1

Force balance on pendant atom $3k$:

$$\mathbf{F}^{B}_{3k,3k-1} = -\sum_{j \neq 3k} \mathbf{F}^{NB}_{3k,j} \quad (B.5)$$

Torque balance on pendant atom $3k$:

$$\boldsymbol{T}^{B}_{3k,3k-1} = \mathbf{0} \quad (B.6)$$

Force balance on pendant atom $3k + 1$:

$$\mathbf{F}^{B}_{3k+1,3k-1} = \sum_{j \neq 3k+1} \mathbf{F}^{NB}_{3k+1,j} \quad (B.7)$$

Torque balance on pendant atom $3k + 1$:

$$\boldsymbol{T}^{B}_{3k+1,3k-1} = \mathbf{0} \quad (B.8)$$

Force balance on pendant bond $(3k - 1, 3k)$:

$$\mathbf{F}^{B}_{3k-1,3k} = -\mathbf{F}^{B}_{3k,3k-1} \quad (B.9)$$

Torque balance on pendant bond $(3k - 1, 3k)$:

$$(-\boldsymbol{T}^{B}_{3k,3k-1}) + (\mathbf{r}_{3k} - \mathbf{r}_{3k-1}) \times (-\mathbf{F}^{B}_{3k,3k-1}) + (-\boldsymbol{T}^{B}_{3k-1,3k}) = \mathbf{0}$$

and

$$\boldsymbol{T}^{B}_{3k-1,3k} = -\boldsymbol{T}^{B}_{3k,3k-1} - (\mathbf{r}_{3k} - \mathbf{r}_{3k-1}) \times \mathbf{F}^{B}_{3k,3k-1} \quad (B.10)$$

Force balance on pendant bond $(3k - 1, 3k + 1)$:

$$\mathbf{F}^{B}_{3k-1,3k+1} = -\mathbf{F}^{B}_{3k+1,3k-1} \quad (B.11)$$

Torque balance on pendant bond $(3k - 1, 3k + 1)$:

$$(-\boldsymbol{T}^{B}_{3k+1,3k-1}) + (\mathbf{r}_{3k+1} - \mathbf{r}_{3k-1}) \times (-\mathbf{F}^{B}_{3k+1,3k-1}) + (-\boldsymbol{T}^{B}_{3k-1,3k+1}) = \mathbf{0}$$

and

$$\boldsymbol{T}^{B}_{3k-1,3k+1} = -\boldsymbol{T}^{B}_{3k+1,3k-1} - (\mathbf{r}_{3k+1} - \mathbf{r}_{3k-1}) \times \mathbf{F}^{B}_{3k+1,3k-1} \quad (B.12)$$

Force balance on skeletal atom $3k - 1$:

$$\mathbf{F}^{B}_{3k-1,3k+2} = -\{\sum_{j \neq 3k-1} \mathbf{F}^{NB}_{3k-1,j} + \mathbf{F}^{B}_{3k-1,k_1} + \mathbf{F}^{B}_{3k-1,3k} + \mathbf{F}^{B}_{3k-1,3k+1}\}$$

where

$$k_1 = \max(1, 3k - 4) \quad (B.13)$$

Torque balance on skeletal atom $3k - 1$:

$$\boldsymbol{T}^{B}_{3k-1,3k+2} = -\{\boldsymbol{T}^{B}_{3k-1,k_1} + \boldsymbol{T}^{B}_{3k-1,3k} + \boldsymbol{T}^{B}_{3k-1,3k+1}\}$$

where

$$k_1 = \max(1, 3k - 4) \quad (B.14)$$

Force balance on skeletal bond $k + 1$:

$$\mathbf{F}^{B}_{3k+2,3k-1} = -\mathbf{F}^{B}_{3k-1,3k+2} \quad (B.15)$$

Torque balance on skeletal bond $k + 1$:

$$(-\boldsymbol{T}^{B}_{3k+2,3k-1}) + (\mathbf{r}_{3k-1} - \mathbf{r}_{3k+2}) \times (-\mathbf{F}^{B}_{3k-1,3k+2}) + (-\boldsymbol{T}^{B}_{3k-1,3k+2}) = \mathbf{0}$$

or

$$\boldsymbol{T}^{B}_{3k+2,3k-1} = -\boldsymbol{T}^{B}_{3k-1,3k+2} - (\mathbf{r}_{3k-1} - \mathbf{r}_{3k+2}) \times \mathbf{F}^{B}_{3k-1,3k+2} \quad (B.16)$$

Axial torque balance along skeletal bond $k + 1$ (see eq 61):

$$\boldsymbol{T}^{B}_{3k+2,3k-1} \cdot \frac{\mathbf{r}_{3k-1} - \mathbf{r}_{3k+2}}{|\mathbf{r}_{3k-1} - \mathbf{r}_{3k+2}|} = \left.\frac{dU\varphi}{d\varphi}\right|_{\varphi=\varphi_{k+1}} \quad (B.17)$$

For (B.5)–(B.16) the index k runs from 1 to $2x - 1$. For (B.17) it runs from 1 to $2x - 2$.

Segment 2x

Torque balance on atom $6x - 1$:

$$\boldsymbol{T}^{B}_{6x-1,6x-4} = \mathbf{0} \quad (B.18)$$

Nonbonded interatomic interaction forces are functions of interatomic distances. For any significantly interacting pair (i,j) we have, according to (60)

$$\mathbf{F}^{NB}_{ij} = \left.\frac{dU^{NB}_{ij}}{dr}\right|_{r=|\mathbf{r}_i - \mathbf{r}_j|} \frac{\mathbf{r}_j - \mathbf{r}_i}{|\mathbf{r}_j - \mathbf{r}_i|} \quad (B.19)$$

Moreover, as shown in Appendix 1 to ref 1, all interatomic distance vectors are analytically expressible in terms of the microscopic degrees of freedom. Symbolically

$$\mathbf{r}_j - \mathbf{r}_i = f(\psi, \varphi; \mathbf{a}_x, \mathbf{a}_y, \mathbf{a}_z) \quad (B.20)$$

Equations B.19 and B.20 remain valid when the minimum image convention is imposed.

Equations B.1–B.20 are a complete set of independent balance equations.

We use (B.19) and (B.20) to directly substitute all nonbonded forces $\mathbf{F}^{NB}_{ij}$ and interatomic distance vectors $\mathbf{r}_j - \mathbf{r}_i$ appearing in (B.1)–(B.18) in terms of the microscopic degrees of freedom (ψ, φ). Consider now the system of (B.1)–(B.18) after this substitution. A count of the unknowns appearing in this system yields

components of bonded forces $\mathbf{F}^{B}_{ij}$	$6(6x - 2)$
components of bonded torques $\boldsymbol{T}^{B}_{ij}$	$6(6x - 2)$
microscopic degrees of freedom ψ, φ	$2x + 1$
total number of unknowns	$74x - 23$

A count of the number of equations gives

balances (B.1)–(B.4)	12
balances (B.5)–(B.16)	$36(2x - 1)$
projected torque balances (B.17)	$2x - 2$
balances (B.18)	3
total number of equations	$74x - 23$

The number of equations is thus equal to the number of unknowns and, in principle, the microscopic degrees of freedom, ψ, φ are determinable from the solution of this system. The minimum energy requirement (eq 47) is obtained by elimination of the variables $\mathbf{F}^{B}_{ij}$ and $\boldsymbol{T}^{B}_{ij}$ from the system of (B.1)–(B.18). It involves only $2x + 1$ variables and is thus much preferable to solve in practice.

Once we know the microscopic degrees of freedom ψ and φ (as we do for every one of the undeformed and deformed structures in this paper), the system of deformed balance equations becomes *overdetermined* and $2x + 1$ of the equations can be used as consistency tests. As such we chose here to use the $2x - 2$ projected torque balances (eq

B.17), together with the three torque balances on the last atom (eq B.18).

To obtain all forces and torques in a given structure we first compute all nonbonded forces (hence, the total nonbonded force on each atom) via (B.19). We then solve (B.1)–(B.16) sequentially, in the order they have been written above, to get all bonded forces and torques. In the course of this segment-by-segment solution of the balance equations we test for consistency via (B.17) and (B.18).

We found that the projected torques on the left-hand side of (B.17) and (B.18) deviate from the derivatives $U'\varphi(\varphi_{k+1})$ by a relative error of less than 10^{-5}, which confirms the excellent performance of the minimizations.

Appendix C: Equivalence of the Force and Virial Theorem Approaches

The *force approach* rests on a calculation of the "face forces" $\mathbf{F}_f$ exerted on the interior of the cube by its surroundings through each of its faces, f. We denote by $f = 1$ the face parallel to the edge vectors $\mathbf{a}_y$ and $\mathbf{a}_z$ and containing the origin $\mathbf{0}$, by $f = 3$ the face parallel to the edge vectors $\mathbf{a}_z$ and $\mathbf{a}_x$ and containing the origin $\mathbf{0}$, and by $f = 5$ the face parallel to the edge vectors $\mathbf{a}_x$ and $\mathbf{a}_y$ and containing the origin $\mathbf{0}$.

$$\mathbf{n}_1 = -\frac{\mathbf{a}_y \otimes \mathbf{a}_z}{S_1}, \qquad S_1 = |\mathbf{a}_y \otimes \mathbf{a}_z| \tag{C.1a}$$

$$\mathbf{n}_3 = -\frac{\mathbf{a}_z \otimes \mathbf{a}_x}{S_3}, \qquad S_3 = |\mathbf{a}_z \otimes \mathbf{a}_x| \tag{C.1b}$$

$$\mathbf{n}_5 = -\frac{\mathbf{a}_x \otimes \mathbf{a}_y}{S_5}, \qquad S_5 = |\mathbf{a}_x \otimes \mathbf{a}_y| \tag{C.1c}$$

From (63), applied for the faces 1, 3, and 5, we have, in matrix notation (all vectors taken as column vectors)

$$\mathbf{F} = [\mathbf{F}_1 \quad \mathbf{F}_3 \quad \mathbf{F}_5] = \sigma^T[\mathbf{n}_1 S_1 \quad \mathbf{n}_3 S_3 \quad \mathbf{n}_5 S_5] = \sigma^T \mathbf{S}$$

and

$$\sigma^T = \mathbf{F}\mathbf{S}^{-1} \tag{C.2}$$

Using (C.1) one can readily calculate $\mathbf{S}^{-1}$ as

$$\mathbf{S}^{-1} = -\frac{1}{V}\begin{bmatrix} \mathbf{a}_x^T \\ \mathbf{a}_y^T \\ \mathbf{a}_z^T \end{bmatrix} \tag{C.3}$$

Therefore, from (C.2) and (C.3)

$$\sigma = -\frac{1}{V}[\mathbf{a}_x \mathbf{a}_y \mathbf{a}_z]\begin{bmatrix} \mathbf{F}_1^T \\ \mathbf{F}_2^T \\ \mathbf{F}_3^T \end{bmatrix} \tag{C.4}$$

or, equivalently

$$\sigma_{LM} = -\frac{1}{V}(a_{x,L}F_{1,M} + a_{y,L}F_{3,M} + a_{z,L}F_{5,M}) \tag{C.5}$$

$\mathbf{F}_1$ is the sum of all forces exerted on cube atoms from images of other cube atoms that lie across face 1. Let (h_j, k_j, l_j) denote the continuation coefficients of an atom j of the cube (in ref 1 the quantities h, k, l have been symbolized by λ, μ, and ν respectively). Let $j_{\min}(i)$ be that image of atom j of the cube that lies closest to atom i (minimum image of j with respect to i). By the minimum image convention[1,25] only minimum image pairs interact. We have

$$\mathbf{F}_1 = \sum_i \sum_j \mathbf{F}_{ij}^{\min} = \frac{1}{2}\left[\sum_i \sum_j \mathbf{F}_{ij}^{\min} + \sum_j \sum_i \mathbf{F}_{ji}^{\min}\right]$$

(i, j in cube, i and $j_{\min}(i)$ lie across face 1; i, j in cube, i and $j_{\min}(i)$ lie across face 1; i, j in cube, j and $i_{\min}(j)$ lie across face 1)

Now, if j and $i_{\min}(j)$ lie across face 1, $j_{\min}(i)$ and i will lie across face 2, which is the face opposite to face 1. Then

$$\mathbf{F}_1 = \frac{1}{2}\left[\sum_i \sum_j \mathbf{F}_{ij}^{\min} - \sum_i \sum_j \mathbf{F}_{ij}^{\min}\right] =$$

(i, j in cube, i and $j_{\min}(i)$ lie across face 1; i, j in cube, i and $j_{\min}(i)$ lie across face 2)

$$\frac{1}{2}\left[\sum_i \sum_j \mathbf{F}_{ij}^{\min} - \sum_i \sum_j \mathbf{F}_{ij}^{\min}\right] = \frac{1}{2}\left[\sum_i \sum_j \mathbf{F}_{ij}^{\min} - \sum_i \sum_j \mathbf{F}_{ij}^{\min}\right]$$

(i, j in cube, j and $j_{\min}(i)$ lie across face 1; i, j in cube, j and $j_{\min}(i)$ lie across face 2; i, j in cube, $h_j - h_{j\min(i)} = +1$; i, j in cube, $h_j - h_{j\min(i)} = -1$)

and, since the possible values of the difference $h_j - h_{j_{\min}(i)}$ are -1, 0, and 1,[25] we have

$$\mathbf{F}_1 = \frac{1}{2}\sum_i \sum_j [h_j - h_{j_{\min}(i)}]\mathbf{F}_{ij}^{\min} \tag{C.6}$$

and similarly for $\mathbf{F}_3$ and $\mathbf{F}_5$. Equation C.5 then assumes the form

$$\sigma_{LM} = -\frac{1}{2V}\sum_i \sum_{j\neq i} [(h_j - h_{j_{\min}(i)})a_{x,L} + (k_j - k_{j_{\min}(i)})a_{y,L} +$$

$$(l_j - l_{j_{\min}(i)})a_{z,L}]F_{ij,M}^{\min} = -\frac{1}{2V}\sum_i \sum_{j\neq i} (r_j - r_{j_{\min}(i)})_L F_{ij,M}^{\min}$$

$$= -\frac{1}{2V}\sum_i \sum_{j\neq i} (r_{j,L} - r_{i,L})F_{ij,M}^{\min} -$$

$$\frac{1}{2V}\sum_i \sum_{j\neq i} (r_{i,L} - r_{j,L})_{\min} F_{ij,M}^{\min} \tag{C.7}$$

The first term in (C.7) can further be written

$$-\frac{1}{2V}\sum_i \sum_{j\neq i} (r_{j,L} - r_{i,L})F_{ij,M}^{\min} =$$

$$\frac{1}{2V}\sum_i \sum_{j\neq i} r_{j,L}F_{ji,M}^{\min} + \frac{1}{2V}\sum_i \sum_{j\neq i} r_{i,L}F_{ij,M}^{\min} =$$

$$\frac{1}{V}\sum_i \sum_{j\neq i} r_{i,L}F_{ij,M}^{\min} = \frac{1}{V}\sum_i r_{i,L}\sum_{j\neq i} F_{ij,M}^{\min} = 0 \tag{C.8}$$

because the condition of detailed mechanical equilibrium around atom i dictates that $\sum_{j\neq i} F_{ij,M}^{\min} = 0$.

We are thus left, from (C.7) and (C.8), with the expression

$$\sigma_{LM} = -\frac{1}{2V}\sum_i \sum_{j\neq i} (r_{i,L} - r_{j,L})_{\min} F_{ij,M}^{\min}$$

which is exactly the *virial theorem expression* (eq 65).

Appendix D: Sensitivity Analysis

To test the sensitivity of the model estimates with respect to the potential energy parameters employed we subjected one of the undeformed structures to a new relaxation and to tension and shear deformations using a slightly different set of van der Waals radii. All computations presented in the main body of this paper have been performed by using the potential parameters employed by Suter and Flory[31] in their development of a rotational isomeric state scheme for PP.[1] These van der Waals radii are the "base case" radii listed in Table II. For the sensitivity analysis runs, values were changed to the ones suggested by Bondi (p 2 of ref 15) and by Tadokoro (p 326 of ref 27), listed as "perturbed case" in Table II. The two sets differ by 0.1 Å for H and C only, reflecting the small degree of uncertainty that exists regarding the potential parameters.

The particular structure examined in the sensitivity runs was somewhat anomalous, since it displayed a negative ratio α_P/κ_T and considerably higher than average elastic coefficients. The influence of changing van der Waals radii

on the theoretical estimates of various properties is displayed in Table III. One sees that the solubility parameter and the elastic constants change relatively little but that the ratio α_P/κ_T (hence, our estimate of the thermal expansion coefficient) exhibits a very strong dependence on the atomic radii, jumping from its original negative value to a positive one (which actually is close to the experimental ratio α_P/κ_T for glassy atactic polypropylene under the appropriate conditions).

Thus, small uncertainties in the potential parameters can well be tolerated in predicting the solubility and the elastic constants with our approach but appear to render our estimate of the thermal expansion coefficient unreliable.

Registry No. Polypropylene (homopolymer), 9003-07-0.

References and Notes

(1) Theodorou, D. N.; Suter, U. W. *Macromolecules* **1985**, *18*, 1467-1478.
(2) Pastine, D. J. *J. Chem. Phys.* **1968**, *49*, 3012-22.
(3) Tashiro, K.; Kobayashi, M.; Tadokoro, H. *Macromolecules* **1977**, *10*, 413-20.
(4) Tashiro, K.; Kobayashi, M.; Tadokoro, H. *Macromolecules* **1978**, *11*, 908-13.
(5) Haward, R. N.; MacCallum, J. R. *Polymer* **1971**, *12*, 189-93.
(6) Van Krevelen, D. W.; Hoftyzer, P. J. "Properties of Polymers—Their Estimation and Correlation with Chemical Structure"; Elsevier: Amsterdam, 1976.
(7) Yannas, I. V. "Molecular Interpretation of Deformation in Glassy Polymers" in "Proceedings of the International Symposium on Macromolecules, Rio de Janeiro, July 26-31"; Mano, Ed.; Elsevier: Amsterdam, 1975.
(8) Yannas, I. V.; Luise, R. R. *J. Macromol. Sci., Phys.* **1982**, *B21*, 443-74. Yannas, I. V.; Luise, R. R. "The Strophon Theory of Deformation of Glassy Amorphous Polymers: Application to Small Deformations" in "The Strength and Stiffness of Polymers"; Zachariades, A. E.; Porter, R. S., Eds.; Marcel Dekker: New York, 1983.
(9) Maeda, K.; Takeuchi, S. *Philos. Mag. A* **1981**, *44*, 643-56.
(10) Srolovitz, D.; Vitek, V.; Egami, T. *Acta Metall.* **1983**, *31*, 335-52.
(11) Weiner, J. H. "Statistical Mechanics of Elasticity"; Wiley: New York, 1983.
(12) Callen, H. B. "Thermodynamics"; Wiley: New York, 1960.
(13) Koppelmann, J.; Leder, H.; Royer, F. *Colloid and Polym. Sci.* **1979**, *257*, 673-88.
(14) Gō, N.; Scheraga, H. A. *Macromolecules* **1976**, *9*, 535-43.
(15) Bondi, A. "Physical Properties of Molecular Crystals, Liquids and Glasses"; Wiley: New York, 1968.
(16) Zallen, R. "The Physics of Amorphous Solids"; Wiley Interscience: New York, 1983.
(17) Yannas, I. V. "Introduction to Polymer Science and Engineering—A Set of Lecture Notes", Part 2; MIT Press: Cambridge, MA; 1981.
(18) Reichl, L. E. "A Modern Course in Statistical Physics"; University of Texas Press: Austin, 1980.
(19) Born, M.; Huang, K. "Dynamical Theory of Crystal Lattices"; Clarendon Press: Oxford, 1954; Chapter II.
(20) Kaufmann, H. S.; Falcetta, J. J. "Introduction to Polymer Science and Technology"; Wiley: New York, 1977.
(21) Zakin, J. L.; Simha, R.; Hershey, H. C. *J. Appl. Polym. Sci.* **1966**, *10*, 1455-73.
(22) Abramowitz, M.; Stegun, I. A. "Handbook of Mathematical Functions"; 10th printing; National Bureau of Standards: Washington, DC, 1972.
(23) Simha, R.; Roe, J. M.; Nanda, V. S. *J. Appl. Phys.* **1972**, *43*, 4312-7.
(24) Weaire, D.; Ashby, M. F.; Logan, J.; Weins, M. J. *Acta Metall.* **1971**, *19*, 779-88.
(25) Theodorou, D. N.; Suter, U. W. *J. Chem. Phys.* **1985**, *82*, 955-66.
(26) Swenson, R. J. *Am. J. Phys.* **1983**, *51*, 940-2.
(27) Tadokoro, H. "Structure of Crystalline Polymers"; Wiley: New York, 1979.
(28) Sauer, J. A.; Wall, R. A.; Fuscillo, N.; Woodward, A. E. *J. Appl. Phys.* **1958**, *29*, 1385-9.
(29) Flory, P. J. "Principles of Polymer Chemistry"; Cornell University Press: Ithaca, NY, 1953.
(30) Flory, P. J. "Statistical Mechanics of Chain Molecules"; Wiley Interscience: New York, 1969.
(31) Suter, U. W.; Flory, P. J. *Macromolecules* **1975**, *8*, 765-76.

Theoretical Study of the Influence of Strain Rate and Temperature on the Maximum Strength of Perfectly Ordered and Oriented Polyethylene

Yves Termonia,* Paul Meakin, and Paul Smith

Central Research and Development Department, Experimental Station, E. I. du Pont de Nemours and Company, Incorporated, Wilmington, Delaware 19898.
Received June 18, 1985

ABSTRACT: The stochastic model for failure of perfectly ordered and oriented polymer filaments, previously introduced, is used for a theoretical study of the influence of strain rate and temperature on the maximum tensile strength of polyethylene of two (monodisperse) molecular weights (2.2×10^4, 3.3×10^5). The model predicts polyethylene to display a strong strain rate and temperature dependence of the maximum strength; higher strength is predicted at low temperatures and at high strain rates. At strain rates exceeding 10^4 min^{-1} the theoretical ultimate strength (~24 GPa) is recovered for both molecular weights studied. At high strain rates and at low temperatures, polyethylene of both high and low molecular weight fails in a brittle mode and fracture is accompanied by a substantial amount of C-C bond cleavage. Failure at low strain rates and/or high temperatures is found to be creep-like and is dominated by secondary bond breakage. The effects of the strain rate and, to a lesser extent, of the temperature are more pronounced for low than for high molecular weight polyethylene. Good qualitative agreement is found between the present theoretical work and related experimental data.

1. Introduction

In a previous theoretical study,[1] we developed a stochastic model based on the kinetic theory of fracture,[2,3] to describe failure of perfectly oriented and ordered polymer filaments. The model was applied to polyethylene, and it was used to investigate the effect of the molecular weight on the maximum tensile strength at constant (room) temperature and at a fixed strain rate (1 min^{-1}).

It is well-known that the test temperature and strain rate, among other testing conditions, have a major effect on the measured fiber properties.[4,5] Employing the previously introduced model,[1] we explore here the influence of both the strain rate and the temperature on the tenacity

0024-9297/86/2219-0154$01.50/0